Spectral Efficiency and Outage Performance Evaluation of Measured Vehicular Communication Radio Channels

Author: Arrate Alonso Gómez
Director 1: Alberto González Salvador / Gema Piñero Sipán
Director 2: Christoph F. Mecklenbräuker / Alexander Paier

Resumen

Los sistemas cooperativos para entornos vehiculares tienen la capacidad de mejorar tanto la seguridad en carretera, como la gestión del tráfico. Tienen como base la norma del estándar de comunicaciones inalámbrico de red de área local (*Wireless Local Area Network,* WLAN) para el uso comunicaciones vehiculares (*Vehicle-to-Vehicle/Infrastructure,* V2I), denominada IEEE 802.11p, la cual se está desarrollando actualmente, y que dará lugar a la nueva tecnología de comunicaciones entre vehículos e infraestructura WAVE (*Wireless Access in Vehicular Environments*). Funcionando en el rango de frecuencias de 5.850 a 5.925 GHz, los sistemas WAVE adoptan la técnica de multiplexación OFDM (*Orthogonal Frequency Division Multiplexing*) y alcanzan tasas de transmisión de datos en el rango de 6 a 27 Mbps. El estudio del canal es clave para conocer el efecto de las condiciones de propagación reales sobre la transmisión. Habrá que tener en cuenta que en entornos de comunicaciones vehiculares se da la propagación con línea de visión directa *(Line of Sight,* LoS*)*, por lo que a la hora de caracterizar el canal, habrá que considerar tanto el desvanecimiento Rayleigh como el desvanecimiento Ricean. Este estudio se hará a partir del procesado de la función de transferencia del canal obtenido para diferentes escenarios durante la campaña de medidas realizada en Lund, Suecia. en 2007 por la Universidad Técnica de Viena. El sistema radio utilizado considera múltiples antenas, es decir, el canal es *Multiple-Input Multiple-Output* (MIMO), dado que gracias a la diversidad consigue un mayor rendimiento. De cara a analizar el efecto de las condiciones de propagación sobre el rendimiento alcanzable, se caracterizará el canal mediante el *Power Delay Profile* (PDP) y el perfil de *Path Loss*. A continuación se estudiarán más en detalle los canales MIMO con desvanecimiento Ricean, cruciales para las comunicaciones *Vehicle-to-Vehicle, (*V2V).

Autor: Alonso Gómez, Arrate, email: aalonso@nt.tuwien.ac.at
Director 1: González Salvador, Alberto, email: agonzal@dcom.upv.es
Director 2: Christoph F. Mecklenbräuker, email: cfm@nt.tuwien.ac.at
Fecha de entrega: 09-12-09

En estos canales hay una tasa de datos crítica (R_{CRIT}) dependiente de una relación señal a ruido (*Signal-to-Noise Ratio,* SNR) bajo la cual la transmisión de datos con cero *outage* es posible, de manera que el canal se comporta como un canal con ruido aditivo gaussiano (*Additive White Gaussian Noise*, AWGN). Se analizará la tanto eficiencia espectral en términos de capacidad ergódica y como la probabilidad de *outage* del canal vehicular para diferentes valores de relación señal a ruido.

Abstract

Roadway-vehicle cooperative systems will lead to improve driving safety. These systems relay on a wireless local area network (WLAN) standard for automotive use, called IEEE 802.11p, which is under development in order to implement Wireless Access in Vehicular Environments (WAVE). Operating at 5.850–5.925 GHz, WAVE systems adopt orthogonal frequency-division multiplexing (OFDM) and achieve data rates of 6–27 Mbps. The development of efficient vehicle-to-vehicle (V2V) communications systems requires an understanding of the underlying radio propagation channels in order to analyze the real impact of real-world propagation conditions. Vehicular communication channels are non-stationary, because the conditions of the channel vary abruptly due to the speed of the vehicles. The studied wireless communication scenario is predominantly Line of Sight (LoS) propagation scenario, therefore Rayleigh fading and Ricean fading have to be considered for channel characterization. The reference data to be analyzed have been obtained from a channel sounding campaign carried out by the Vienna University of Technology in Lund, Sweden in 2007. The radio system used for this campaign is a multiple-input multiple-output (MIMO) system. Radio channel parameters such as the power delay profile and the path loss are going to be analyzed in order to study the impact of real-world propagation conditions. Reliability in Ricean MIMO channel is going to be more deeply characterized, as it is crucial for safety related V2V applications. In such channels, there is a SNR-dependent critical data rate (R_{CRIT}) below which signaling with zero outage is possible, and hence the fading channel behaves like an AWGN channel. For the vehicular time variant channel spectral efficiency is going to be evaluated in terms of ergodic capacity and outage performance is also going to be studied by means of outage probability.

Keywords

Vehicular Communications, MIMO systems, Radio channel characterization, Channel Reliability, Spectral Efficiency, Outage Probability

Contents

I. INTRODUCTION **1**

I.1. Dynamics of the vehicular Wireless Channel 2

I.2. MIMO Channel and Signal Model 3

I.3. Outline of the Master Thesis 5

II. WIRELESS LAN ACCORDING TO IEEE 802.11p **7**

II.1. Definition of Key OFDM Parameters 7

II.2. IEEE 802.11p Draft Amendment for Wireless Access in Vehicular Environments 10

III. FADING IN VEHICULAR ENVIRONMENTS **15**

III.1. Fading in Wireless Environment 15

III.2. Statistical Modelling of Fading 17

IV. CHARACTERIZATION OF MIMO CHANNELS IN VEHICULAR ENVIRONMENTS **21**

IV.1. Channel Models for Vehicular Environments 21

IV.2. Characterization Criteria of Measured MIMO Channel in Vehicular Environments 24

V. SPECTRAL EFFICIENCY AND OUTAGE PERFORMANCE IN RICEAN VEHICULAR COMMUNICATION CHANNELS **27**

V.1. Ricean Vehicular Communication Channel 27

V.2. Spectral Efficiency and Outage Performance in Vehicular Communication Channels 29

VI. RESULTS **35**

VI.1. Characterization of the Propagation Scenario 36

VI.2. Spectral Efficiency Evaluation for the Measured Channel 37

VI.3. Outage Performance Evaluation for the Measured Channel 43

VII. SUMMARY AND CONCLUSIONS **45**

ACKNOWLEDGEMENTS **49**

BIBLIOGRAPHY **51**

I. INTRODUCTION

Due to the importance of road safety in recent years the research on Vehicle-to-Vehicle (V2V) and Vehicle-to-Infrastructure (V2I) communication has become a matter of relevance. V2I telematic systems have the potential to make roads safer and their use more efficient. The deployment of real-time services provides users with critical safety-related information. This allows a reduction in the number and the severity of accidents. Furthermore, traffic can be more efficiently managed and congestions can be avoided.

The IEEE 802.11p [1], also known as Wireless Access in Vehicular Environments (WAVE), is an international draft standard for wireless access in vehicular environments. This specification is an extension of the Wireless Local Area Network (WLAN) standard IEEE 802.11, but it operates in the 5.9 GHz frequency band and it has been conceived to provide reliable communication in traffic scenarios. It defines physical (PHY) and medium access control (MAC) layer features for vehicular communications.

By radio channel means, a very important fact to be taken into account in this type of safety-oriented wireless communications is fading. This effect can degrade the performance of wireless communication systems significantly. In order to compensate this effect, multiple-input multiple-output (MIMO) antenna systems provide diversity [2], which provides the receiver with multiple replicas of the transmitted signal and makes it more powerful at the receiver in order to combat the fading. Space-time codes [3] are capable of extracting spatial diversity gain in systems employing multiple antennas at transmitter and receiver without requiring prior channel knowledge at the transmitter. Orthogonal space-time block codes (OSTBC) [4] are particularly attractive, since they produce maximum spatial diversity gain and at the same time decouple the vector detection problem into scalar detection problems, which significantly reduces decoding complexity (at expense of spatial transmission rate, except in the case of the systems with two transmit antennas using the Alamouti scheme [5]).

The performance of any space-time coding scheme strongly depends on the MIMO channel statistics, which in turn depends on the antenna characteristics, height and spacing, and scattering richness. The classical i.i.d. (independent identically distributed) Rayleigh frequency-flat fading MIMO channel model [6] assumes that the elements of the channel matrix are i.i.d. zero-mean circularly symmetric complex Gaussian distributed. However, measurements from [7] reveal that in practice, the MIMO channel deviates significantly from this idealistic behaviour.

In this Master Thesis, an overview of the IEEE 802.11p draft amendment for vehicular communications is presented, as well as a brief review of the vehicular communication channel characteristics, regarding fading and channel models.

After a theoretical study of Ricean MIMO channels for V2X communications, real-world channels from the measurement campaign of Vienna University of Technology are characterized by terms of Power Delay Profile and Path loss. Finally the spectral efficiency and the outage performance of the channel are evaluated by terms of ergodic capacity and outage probability, respectively.

I.1. *Dynamics of the Vehicular Wireless Channel*

In a received signal, the variation of the amplitude of the signal is known as fading. It can be caused by changes in the characteristics of the propagation path with both time in time variant channels and time-invariant channels [8]. In radio communications this cause is named multipath propagation. Finding the rate where the fading pattern changes can help to program the amplifiers in transmitter and receiver in order to have a more robust signal at the receiver.

The dynamics of a wireless channel can be separated into path loss and fading. *Path Loss* is the reduction of power density (attenuation) of an electromagnetic wave as it propagates through space. It depends on many factors like free space loss, refraction, diffraction, reflection, absorption, environment and propagation medium. In vehicle to either vehicle or to infrastructure (V2X) communication, as in the rest of radio communications, a Line of Sight (LoS) path exists if no blockage happens between the transmitter and the receiver. The characteristics for path loss can be defined according to the existence of LoS:

- LoS
- NLoS (Non Line of Sight)

For the LoS case one modelling approach is the two ray path loss model [9] for determining the received signal power level.

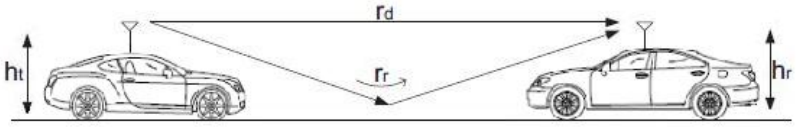

Fig. 1: Two ray path loss model

$$P_r = \frac{P_t G_r G_t}{L(r_d)} \left| D_d \left(\frac{\lambda}{4\pi r_d}\right) + D_r \left(\frac{\lambda}{4\pi r_r}\right) \varrho e^{-j\{k(r_d - r_r)+\phi\}} \right|^2 \qquad (1)$$

In Eq. 1 P_t is the transmission power, G_t and G_r are the gains of the antennas at the transmitters and the receiver, respectively, λ is the wavelength of the propagating signal, r_d and r_r are the path lengths of the direct and reflected signals (see Fig.1), ϕ is the phase rotation due to ground reflection, ϱ is the reflection coefficient, D_d and D_r are the antennas´ directivity coefficients and $L(r_d)$ is the absorption factor (such as in atmosphere $L(r_d) = (d/\lambda)^{\gamma-2}$).

The NLoS case occurs when there is a total obstruction of the path between the transmitter and receiver antenna. This happens in scenarios such as heavy traffic situations, overtaking larger vehicles as trucks or road crossings with buildings obstructing direct LoS between the transmitter and the receiver, for example. In this case, log-distance path loss model is used for NLoS case modelling [10]. Based on this model average received signal power decreases logarithmically with distance, whether in outdoor or indoor radio channels. The average large-scale path loss for an arbitrary Transmitter-Receiver separation is expressed as a function of distance by using path loss exponent γ

$$P_r = P_t G_t G_r \left(\frac{\lambda}{4\pi}\right)^2 \qquad d \leq 1m \qquad (2)$$

$$P_r = P_t G_t G_r \left(\frac{\lambda}{4\pi}\right)^2 \frac{1}{d^\gamma} \quad d > 1m \qquad (3)$$

where d is the distance between the transmitter and the receiver. Exponent γ takes a value between 2.8 and 5.9 [9]. The path loss can be investigated in different scenarios (highway, urban, rural roads) and it is characterized by *Path loss over distance* characteristic. The lognormal variations of the field strength have commonly been attributed to shadowing effects. The effect of fading in wireless environments will be explained more in detail in Chapter III, as introduction to the statistical modelling of each fading.

I.2. *MIMO Channel and Signal Model*

In this section the MIMO channel model basics are introduced, followed by a brief description of the signal model for OSTBCs.

General MIMO Channel Model

In this Master Thesis a Ricean fading MIMO channel is considered for evaluation purposes, with M_T transmit antennas and M_R receive antennas. The corresponding $M_R x M_T$ random channel matrix $\boldsymbol{H} = \bar{\boldsymbol{H}} + \tilde{\boldsymbol{H}}$ is decomposed into the sum of a fixed LoS component $\bar{\boldsymbol{H}} = \mathbb{E}\{\boldsymbol{H}\}$ and a variable (or scattered) component $\tilde{\boldsymbol{H}}$. The channel matrix $\boldsymbol{H}$ is normalized such as in [11]:

$$\mathbb{E}\{tr(\boldsymbol{H}\boldsymbol{H}^H)\} = N = M_R \cdot M_T \qquad (4)$$

$$\mathbb{E}\{\|\boldsymbol{H}\|_F^2\} = \|\bar{\boldsymbol{H}}\|_F^2 + \mathbb{E}\left\{\left\|\tilde{\boldsymbol{H}}\right\|_F^2\right\} \leq N \qquad (5)$$

Furthermore, it is assumed a time-variant frequency-flat channel model for each OFDM carrier (see Eq. 7). In Ricean fading the elements of $\boldsymbol{H}$ are non-identical channels.

The entries of $\boldsymbol{H}$ are modelled as independent random variables, more precisely,

$$\boldsymbol{H} = \sqrt{\frac{K}{K+1}}\bar{\boldsymbol{H}} + \sqrt{\frac{1}{K+1}}\tilde{\boldsymbol{H}} \qquad (6)$$

where $K \geq 0$ denotes the Ricean factor. This can also be considered as a channel model with partial CSIT (Channel State Information at the Transmitter) where the transmitter knows the mean $\bar{\boldsymbol{H}}$ of the channel $\boldsymbol{H}$.

Generally, non-identical channels will result in non-identical channel estimation errors. These estimation errors will consequently affect the performance of the current systems, and even the structure of the existing receiver. Therefore OSTBC in vehicular channels should be considered non identical.

Signal Model

The input-output relation for a single subcarrier is given by,

$$y(t) = \sqrt{\frac{E_S}{M_T}}\boldsymbol{H}(t)s(t) + n(t) \qquad (7)$$

where y denotes the $M_R\ x\ 1$ received signal vector, E_S is the total average energy available at the transmitter over a symbol period, s is the $M_T\ x\ 1$ transmit signal vector, and n is $M_R\ x\ 1$ spatio-temporally white noise with $\mathbb{E}\{nn^H\} = \sigma^2 I_{M_R}$.

I.3. *Outline of the Master Thesis*

This Master Thesis is structured as follows:

In Chapter 2, the Wireless LAN according to IEEE 802.11p is described in order to have a short overview on the layout of the 5.9 GHz channel and key OFDM parameters that are involved in vehicular communication standard. The IEEE 802.11p Draft Amendment for Wireless Access in Vehicular Environment is also studied in terms of PHY and MAC layers.

Chapter 3 is dedicated to the description of fading in vehicular environments, by means of slow fading and fast fading. Special attention will be paid to Ricean and Rayleigh fading distributions.

Chapter 4 introduces the basics about channel modelling, in order to have an overview of how the fading and the environment affect the channel in time and delay domain. Measured MIMO channel and channel characterization criteria for vehicular environments such as Power Delay Profile and Path loss are here introduced.

In Chapter 5 a theoretical study on Ricean MIMO channels for vehicular communications is carried out and the problems of the spectral efficiency analysis and outage performance evaluation are overcome.

Chapter 6 deals with the main contribution of this Master Thesis. In this chapter all the previously presented knowledge is applied to measured vehicle-to-vehicle radio channel data, in order to evaluate the spectral efficiency (bits/s/Hz) and the outage performance (outage probability) of the vehicular communication channel.

Finally summary and conclusions are drawn in Chapter 7.

II. WIRELESS LAN ACCORDING TO IEEE 802.11p

In this section the IEEE 802.11p draft amendment to the IEEE 802.11 standard to add wireless access in vehicular environments is introduced. It is an enhancement to IEEE 802.11, required to support Intelligent Transport Systems (ITS) applications.

II.1. *Definition of Key OFDM Parameters*

The OFDM (Orthogonal Frequency Division Multiplexing) is a digital transmission technique that divides a signal with high data rate into large number of parallel carriers with lower data rates which are transmitted over orthogonal frequency subcarriers.

The physical layer (PHY) structure is the same for IEEE 802.11a and IEEE 802.11p. As it is defined in the draft standard, IEEE 802.11a uses the OFDM technique. The OFDM system provides a wireless LAN and uses 52 subcarriers [12]. 48 subcarriers out of 52 are used for actual transmission, and 4 are pilot subcarriers.

- The *pilot subcarriers* are used for tracing the frequency offset and phase noise.
- The *short training symbols* are located at the beginning of every PHY data packet and are used for signal detection; frequency offset estimation and time synchronization.

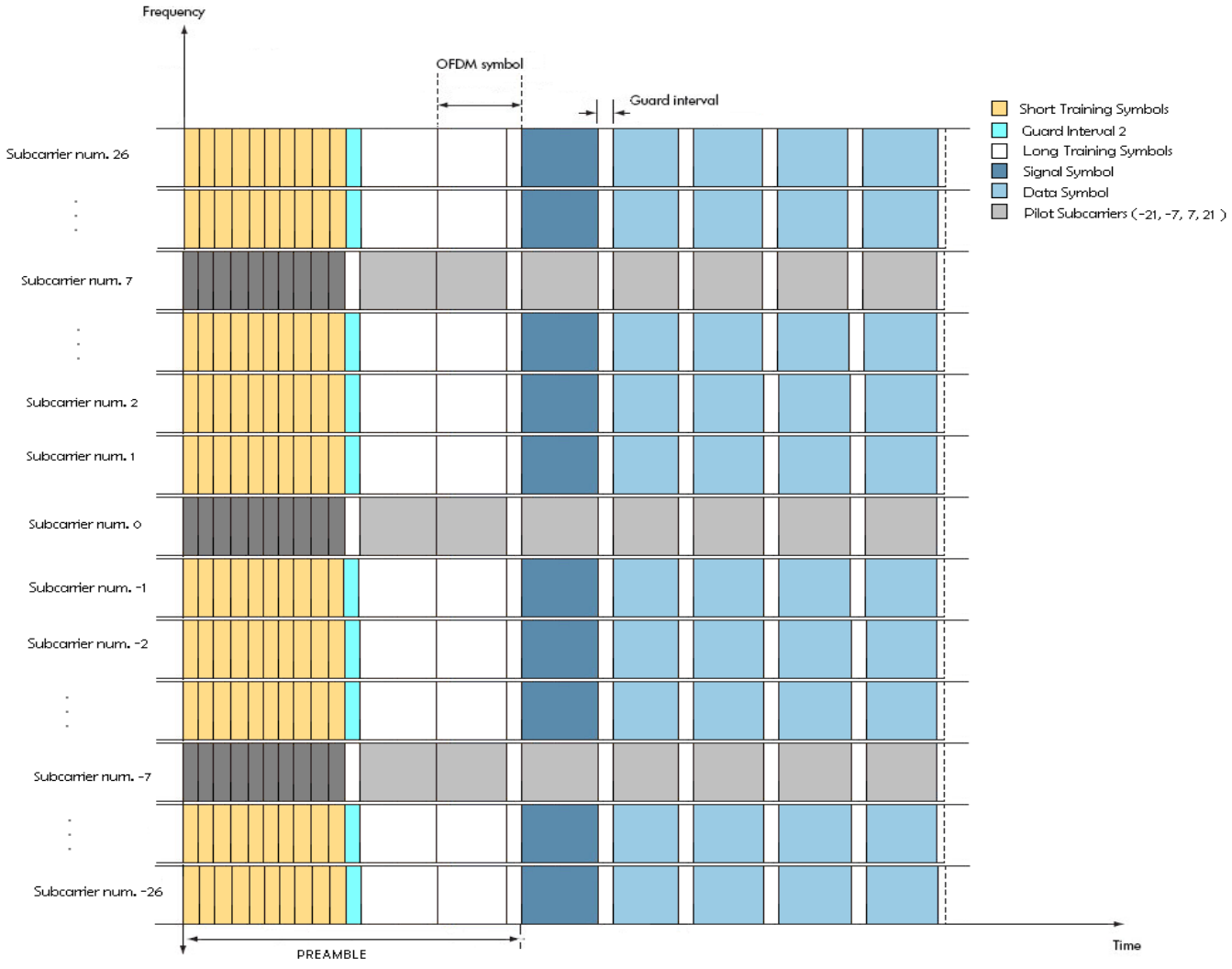

Fig. 2: OFDM Frame structure for IEEE 802.11p in frequency to time domain

- The *long training symbols* are located after the short training symbols and are used for channel estimation and synchronization purposes.
- The *Guard Interval time (GI)*, i.e. cyclic prefix, is located in the OFDM data packet, in order to remove the Inter-Symbol Interference (ISI) caused by the multipath propagation. GI decreases the system capacity and so the received effective signal to interference and noise ratio. Therefore it is important not to make the duration of this factor so long that it affects the efficiency of the transmission.

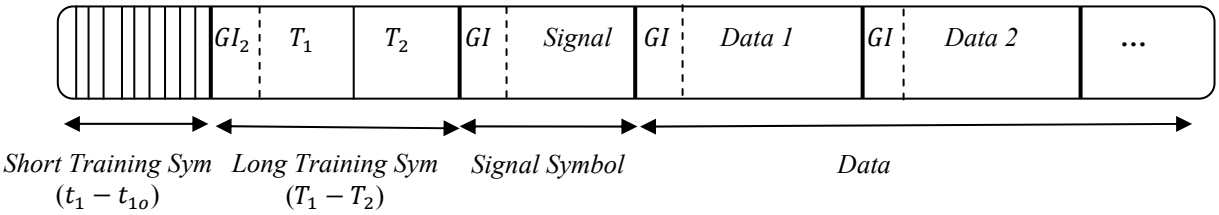

Fig. 3: Packet Structure

Key parameters for the IEEE 802.11a family of OFDM waveform include the length of the cyclic prefix or guard interval, carrier spacing, and the time intervals between channel estimates and corresponding updates to the equalization [13].

Multipath and the Guard Interval

As mentioned before, the IEEE 802.11a protocol uses OFDM transmission format. OFDM is a multicarrier transmission scheme that spreads data over carriers that are spaced at the smallest possible frequency intervals for which the frequencies are orthogonal over the duration of a symbol. Multipath echoes of one symbol that extend into a subsequent symbol may not only cause intersymbol interference (ISI), but can destroy the orthogonality between the carriers. To combat this situation, in practice an OFDM symbol is typically prep ended with a circular extension called cyclic prefix. If the duration of the cyclic prefix is longer than the duration of the echoes, the orthogonality between the symbols and carriers is restored. Thus, the cyclic prefix provides GI for all multiple paths following the first arrival signal. Consequently there should be ensured that the durations of the expected power-delay profiles are shorter than the GI. However, since the GI reduces the channel throughput, the choice of GI represents a trade-off between available data bandwidth and reliability.

Coherence Bandwidth and Carrier Spacing

Multipath effects are also reflected in the frequency domain, resulting in what is known as frequency selective fading. In flat fading case, the bandwidth of the signal is small compared to the scale of variations in the channel response. As a result, the overall amplitude of the signal can vary, but the signal is not distorted. On the other hand, for frequency selective fading, the bandwidth of the signal is large compared to the scale variations in the channel response.

As a result the overall amplitude of the signal is distorted. Equalization can be used to correct the distortion, but it must be updated as the channel changes.

One of the advantages of OFDM is that the carrier spacing can be selected so that each carrier experiences flat fading, even though the spectrum of the OFDM symbol as a whole experiences frequency selective fading. In this case equalization simply consists of multiplying each carrier by a complex constant to correct its amplitude and phase with respect to the others. Since equalization in the IEEE 802.11a PHY is implemented this way, the coherence bandwidth should be greater than the carrier spacing in order to ensure flat fading on each carrier.

Coherence Time and Packet Duration

Vehicular propagation channel changes due to the relative motion between transmitter and receiver, the absolute speeds with respect to the environment, and the motion of the scatterers in the vicinity of the vehicles.

If a narrowband signal is transmitted through the channel, the receiver's signal would experience severe changes in the amplitude and the phase due to such motion. One metric to characterize this time variation is the coherence time, which describes the interval over which the channel can be considered unchanged.

In the PHY specifications of IEEE 802.11a, channel estimation is performed and used to correct flat fading of individual carriers. These estimates are obtained from training sequences in the packet header and are used for the remainder of the packet. Therefore, it is very important to ensure that the duration of the packet is less than the coherence time for the corrections to remain valid.

Doppler Spread and Carrier Spacing

The time-varying properties of the channel manifest themselves in the frequency domain as well. One of the commonly used metrics in the frequency domain is the width of the resulting spectrum, referred as the Doppler spread. To avoid the scenario where a Doppler spread signal leaks into adjacent carriers and causes interference, OFDM carrier spacing must be much larger than the maximum Doppler spread.

PHY parameter	Relevant channel parameters	Criteria for PHY parameter
Guard interval *(GI)*	Maximum excess delay (τ_e)	$GI > \tau_e$
Carrier spacing $(\boldsymbol{D_f})$	Coherence bandwidth (B_c) Doppler spread (B_D)	$B_c > \boldsymbol{D_f} >> B_D$
Interval between channel estimates *(packet length* $\boldsymbol{T_P}$*)*	Coherence Time (T_c)	$\boldsymbol{T_P} < T_c$

Table 1: Key parameters of the IEEE 802.11a family of OFDM waveforms and PHY requirements [13]

In order to prepare the data packet of IEEE 802.11p for high mobility vehicular communications, the bandwidth of the IEEE 802.11p PHY signal is decreased from 20MHz to 10MHz, which means that all parameters in the time domain are doubled. This bandwidth reduction is more suitable for vehicular environments, as the GI is doubled and the best performance is obtained. With 20 MHz bandwidth the GI is not long enough to prevent inter-symbol interference within one radio's own transmissions in the vehicular environments. At lower bandwidths (e.g. 5 MHz), packets tend to be longer, and errors increase due to time variations in the channel degrading equalization. Table 2 illustrates the difference between the IEEE 802.11p PHY and the original IEEE 802.11a.

Different parameters	IEEE 802.11a	IEEE 802.11p	Changes
Bit rate Mb/s	6, 9, 12, 18, 24, 36, 48, 54	3, 4.5, 6, 9, 12, 18, 24, 27	Half
Modulation type	BPSK, QPSK, 16 QAM, 64 QAM	BPSK, QPSK, 16 QAM, 64 QAM	No change
Code rate	1/2, 2/3, 1/4	1/2, 2/3, 1/4	No change
Number of subcarriers	52	52	No change
Symbol duration	4 µs	8 µs	Double
Guard time	0.8 µs	1.6 µs	Double
FFT Period	3.2 µs	6.4 µs	Double
Preamble duration	16 µs	32 µs	Double
Subcarrier frequency spacing	0.3125 MHz	0.15625 MHz	Half

Table 2: Key parameters of IEEE 802.11p PHY and IEEE 802.11a PHY [9]

Moreover, no high bandwidth would be required to run safety-related applications, which are the ones that are currently under development for vehicular communications scenarios.

II.2. *IEEE 802.11p Draft Amendment for Wireless Access in Vehicular Environments*

Definition of European and North American 5.9 GHz Channel Layout

The Federal Communications Commission (FCC) of the US has allocated 75 MHz bandwidth at 5.855−5.925 GHz for the Intelligent Transportation System (ITS). This bandwidth is divided into seven channels of 10MHz, as shown in Fig. 4, and consists of one Control Channel (CCH) and six service channels (SCH). IEEE 802.11p, in the US also called DSRC (Dedicated Short Range Communication), has been adopted as the technique to offer ITS services on this frequency band.

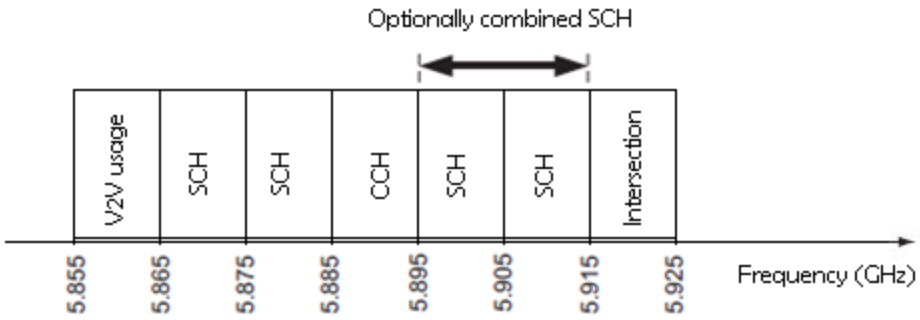

Fig. 4: Frequency allocation of DSRC/IEEE 802.11p in the US [14]

In Europe, after investigations, a 30MHz channel is recommended for road safety applications (5875−5905 MHz), and further 20 MHz (5905−5925 MHz) are suggested to be considered for future ITS expansion [15]. The 30MHz channel is divided into the SCH and CCH [15]:

1. SCH1 (5.875−5.885 GHz) will be used for safety messages with lower priority than CCH and traffic efficiency applications.
2. SCH2 (5.895−5.905 GHz) will be used for short distance transmissions; this results in lower interference for SCH1 and CCH, because of the lower transmit power.
3. CCH (5.885−5.895 GHz) will be used for high priority safety messages and beacons.

The further 20MHz (5.905−5.925 GHz) could be used in several ways. The channel usage efficiency can be increased by using the lower part as a SCH with low transmit power similar to SCH2, and the higher part as a SCH with high transmit power similar to SCH1. The proposed European frequency allocation for ITS applications is illustrated in Fig.5.

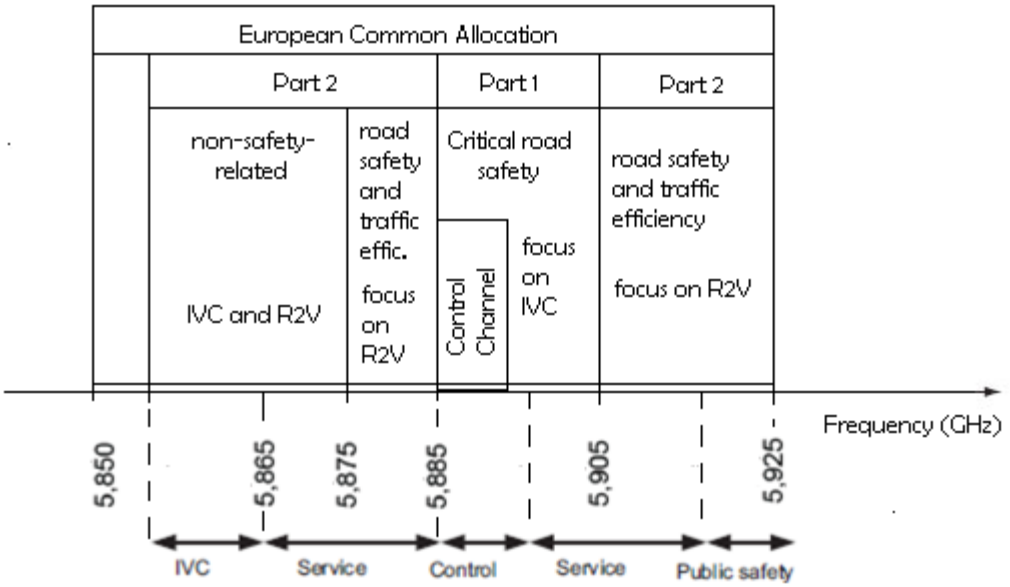

Fig. 5: Proposed ITS spectrum allocation in Europe [15]

The IEEE 802.11p standard

The IEEE 802.11p standard is meant to [14]:

- Describe the functions and services required by WAVE-conformant stations to operate in a rapidly varying environment and exchange messages without having to join a Basic Service Set (BSS), as in the traditional IEEE 802.11 use case. IEEE 802.11p is a peer-to-peer communication scenario.
- Define the WAVE signalling technique and interference functions that are controlled by the IEEE 802.11 MAC.

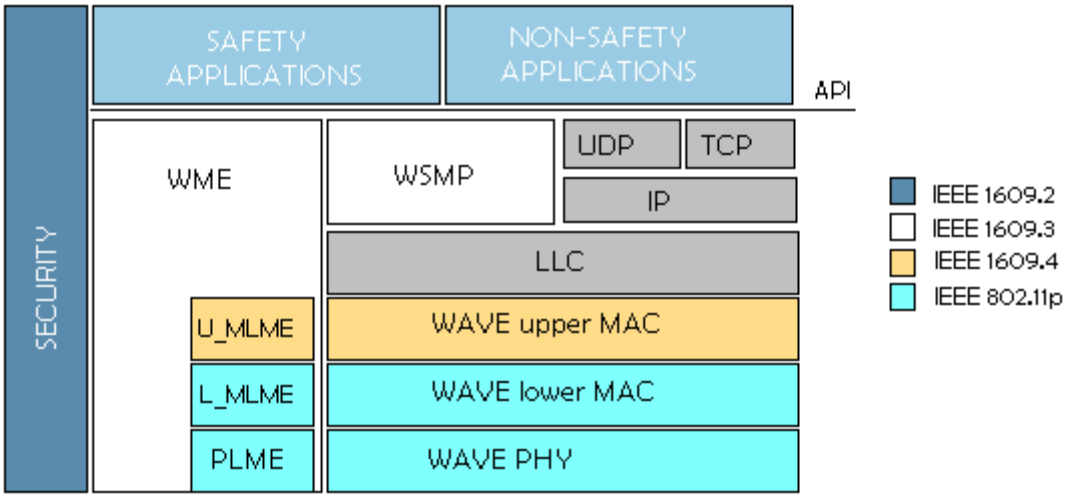

Fig. 6: DSRC standards and communication stack [14]

As shown in Fig. 6, IEEE 802.11p WAVE is only a part of the group of standards related to all layers of protocols for DSRC-based operations. The IEEE 802.11p standard is limited by the scope of IEEE 802.11, which is strictly a MAC and PHY level standard that is meant to work within a single logical channel. All knowledge and complexities related to DSRC channel plan and operational concept are taken care of by upper layer IEEE 1609 standards.

MAC Amendment Details

An infrastructural Basic Service Set is a group of IEEE 802.11 stations anchored by an Access Point (AP) and configured to communicate with each other over air-link. It is usually just referred to as a BSS. The BSS mechanism controls access to an AP´s resources and services, and also allows for a radio to filter out the transmissions from other unrelated radios nearby. A radio first listens for beacon from an AP and then joins the BSS through a number of interactive steps, including authentication and association. The ad-hoc operating mode defined for IEEE 802.11 also follows the similar interactive establishment process of an infrastructure BSS and is called IBSS (Independent BSS). While the name “ad-hoc”, IBSS still carries too much complexity and overhead to be suitable for vehicular communications in the DSRC use cases.

So IEEE 802.11 MAC operations are too time-consuming to be adopted in IEEE 802.11p. Vehicular safety communications use cases demand instantaneous data exchange capabilities and cannot afford scanning channels for the beacon of a BSS and subsequently executing multiple handshakes to establish the communication.

A key amendment introduced by the IEEE 802.11p WAVE is the term "WAVE mode". A station in WAVE mode is allowed to transmit and receive data frames with the wildcard BSSID value (special case of BSSID, which is composed of all "1s") and without the need to belong to a BSS of any kind a priori. This means, two vehicles can immediately communicate with each other upon encounter without any additional overhead as long as they operate in the same channel using the wildcard BSSID.

Even for non-safety communications and services, the overhead of traditional BSS setup may be too expensive. The WAVE standard introduces a new BSS type: WBSS (Wave BSS). A WAVE station uses the demand window beacon, which uses the well known beacon frame and needs not to be periodically repeated, to advertise a WAVE BSS. Such an advertisement is created and consumed by upper layer mechanism above the IEEE 802.11. It contains all the needed information for the receiver stations to understand the services offered in the WBSS in order to decide whether to join, as well as the information needed to configure itself into a member of the WBSS. In other words, a station can decide to join and complete the joining process of a WBSS by only receiving a WAVE advertisement with no further interactions. This approach offers extremely low overhead for WBSS setup by discarding all associations and authentication processes. It requires further mechanisms at uppers layers to manage the WBSS group usage as well as providing security. These mechanisms, however, are out of the scope of the IEEE 802.11.

Given the focus of safety as the key of WAVE, the use of wildcard BSSID is also supported even for a station already belonging to a WBSS (this means expanding wildcard BSSID usage). In other words, a station in WBSS is still in WAVE mode and can still transmit frames with the wildcard BSSID in order to reach all neighbouring stations in cases of safety concerns. Similarly, a station already in a WBSS and having configured its BSSID filter accordingly, can still receive frames from others outside the WBSS with the wildcard BSSID. The ability to send and receive data frames with wildcard BSSID benefits not only safety communications. It is also able to support signalling of future upper layer protocols in this ad-hoc environment.

The distributed service is still available to WAVE devices. Over the air, this simply means that it is possible for data frames to be transmitted with "To DS" and "From DS" bits set to 1. However, the ability for a radio in a WAVE BSS to send and receive data frames with wildcard BSSID introduces complications. It is likely that a radio will be restricted to send a data frame with the wildcard BSSID only if the "To DS" and "From DS" bits are set to 0. This means, radios that are communicating with the context of a WAVE BSS need to send data frames using a known BSSID in order to access DS.

PHY Amendment Details

At PHY level, the philosophy of IEEE 802.11p design is to make the minimum necessary changes to IEEE 802.11 PHY so that WAVE devices can communicate effectively among fast moving vehicles in the roadway environments. While MAC level amendments are fundamentally software updates that are relatively easy to make, PHY level amendment necessarily should be limited in order to avoid designing an entirely new wireless air-link technology. Accordingly, three changes are made:

- 10 MHz Channel: IEEE 802.11 already defines 10MHz wide channels, and it is straightforward in implementation since it mainly involves doubling of all OFDM timing parameters used in regular 20 MHz IEEE 802.11a transmissions. As mentioned before, the key reason for this scaling of IEEE 802.11a is to address the increased RMS delay spread in the vehicular environments. GI at 20 MHz is not long enough to offset the worst case RMS delay spread.
- Improved receiver performance requirements: The nature of closely distributed vehicles on the road creates increased concerned for cross channel interference. Most effective and proper solution to such concerns is through channel management policies and that is completely outside the scope of IEEE 802.11. Nevertheless, IEEE 802.11p introduces some improved receiver performance requirements listed in the proposed standard. Category 1 is mandatory and generally understood to be reachable with today's chip manufacturers. Category 2 is more stringent and optional. It is likely to be more expensive and will be implemented in the few next years.
- Improved transmission mask: Specific to the usage of IEEE 802.11p radios U.S. four spectrum masks are defined that are meant for class A to D operations. These constraints are issued in FCC CFR47 Section 90.377 and Section 95.1509. Generally speaking, these spectrum masks are more stringent than the ones demanded of the current IEEE 802.11 radios. There are debates regarding whether and when chip makers would be able to meet such requirements.

III. FADING IN VEHICULAR ENVIRONMENTS

By now, several aspects have about the vehicular communication protocol and physical channel layout defined in it have been introduced. In this section the fading that occurs in vehicular environments is analyzed and modelled for further processing.

III.1. *Fading in a Wireless Environment*

Multipath propagation comes usually from reflection and scattering from other cars or trucks and diffraction over or around them. In practice the transmitted signal arrives at the receiver via several paths, with different time delays creating a multipath situation. At the receiver, these multipath waves with randomly distributed amplitudes and phases combine to give a resultant signal that fluctuates in time and space. Therefore, a receiver at one location may have a signal that is much different from the signal at another location only a short distance away due to the change in the phase relationship among the incoming radio waves. This situation causes significant fluctuations in the signal amplitude. The phenomenon of random fluctuations in the received signal level is termed as fading.

Whereas the short-term fluctuations in the signal amplitude caused by the local multipath is called *small-scale fading*, and is observed over distances of about half a wavelength, long-term variation in the mean signal level is called *large-scale fading*. The latter effect is a result of movement over distances large enough to cause variations in the overall path between the transmitter and the receiver. Large scale fading is also known as *shadowing,* because these variations in the mean signal level are caused by the mobile unit moving into the shadow of surrounding objects, such as buildings and hills. Because of multipath, a moving receiver can experience several fades in a very short duration. In a more serious case, the vehicle may stop at a location where the signal is in deep fade; in such situation, maintaining good communication becomes an issue of great concern.

Related to small-scale fading [10], there will be two independent fading issues: on one hand small-scale fading based on multipath Time Delay spread and on the other hand based in Doppler Spread. When talking about small-scale fading based on multipath time delay spread, there will be *frequency flat fading* when the bandwidth of the signal is smaller than the bandwidth of the channel, and thus the delay spread is smaller as the symbol period. Alternatively there will be *frequency selective fading* when the bandwidth of the signal is bigger than the bandwidth of the channel, and the delay spread is smaller than the symbol period. The result is time dispersion of the transmitted symbols within the channel arising from these different time delays bringing about intersymbol interference (ISI).

Then again, when mentioning small scale fading according to Doppler spread, there will be *fast fading* when there is a high Doppler spread, thus the coherence time is smaller than symbol period and channel variations are faster than baseband signal variations.

Slow fading will occur with low Doppler spread. Coherence time will be greater than symbol period and channel variations will be slower than baseband variations.

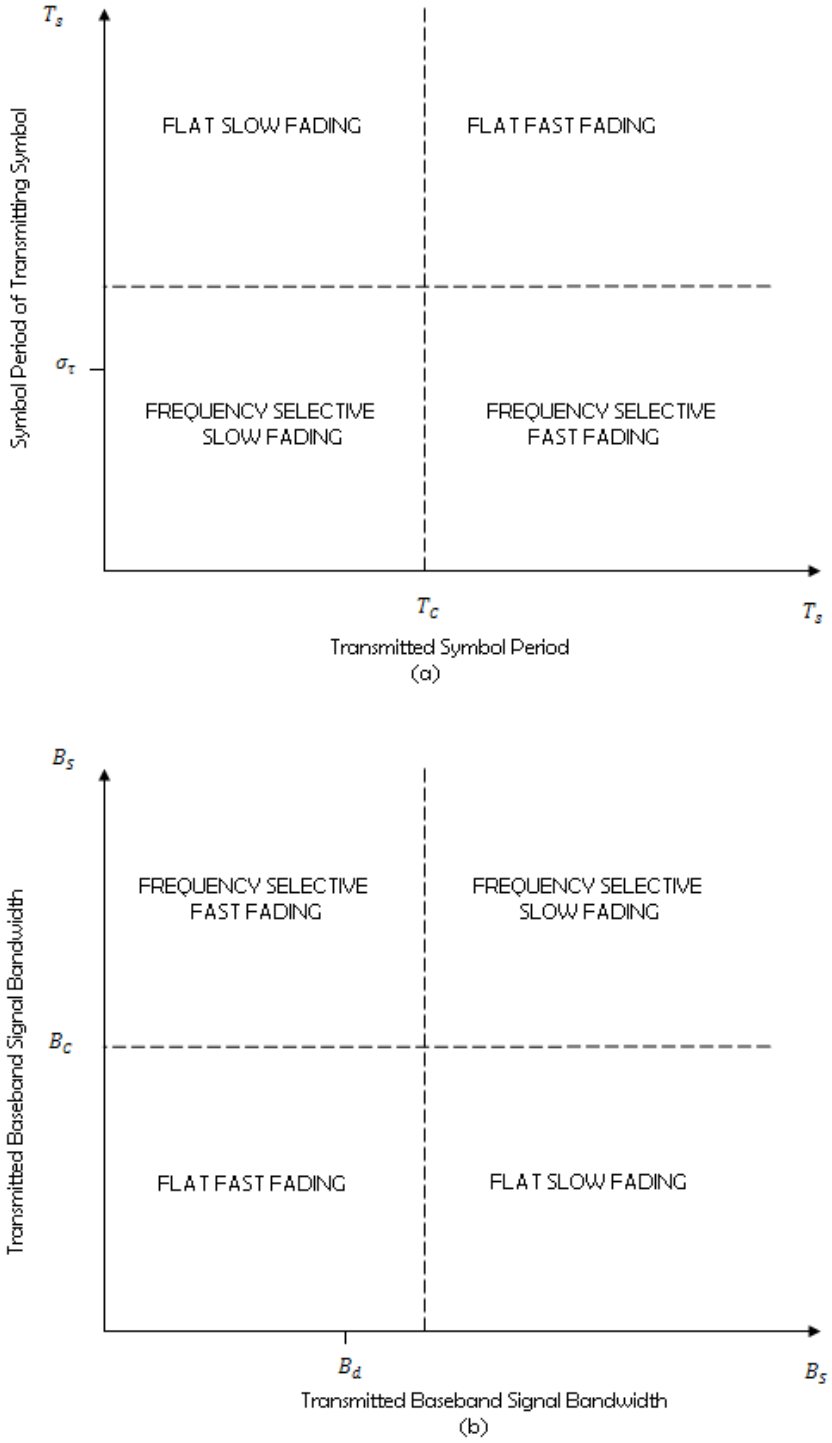

Fig. 7: Matrix illustrating which type of fading is experienced by signals in function of: (a) Symbol period and (b) Baseband signal bandwidth [10]

III.2. *Statistical Modelling of Fading*

To fully understand wireless communications, what happens to the signal as it travels from the transmitter to the receiver has to be analyzed. One of the important aspects of this path between the transmitter and receiver is the occurrence of fading. The radiofrequency signals with appropriate statistical properties can readily be simulated. Statistical testing can subsequently be used to establish the validity of the fading models frequently used in wireless systems.

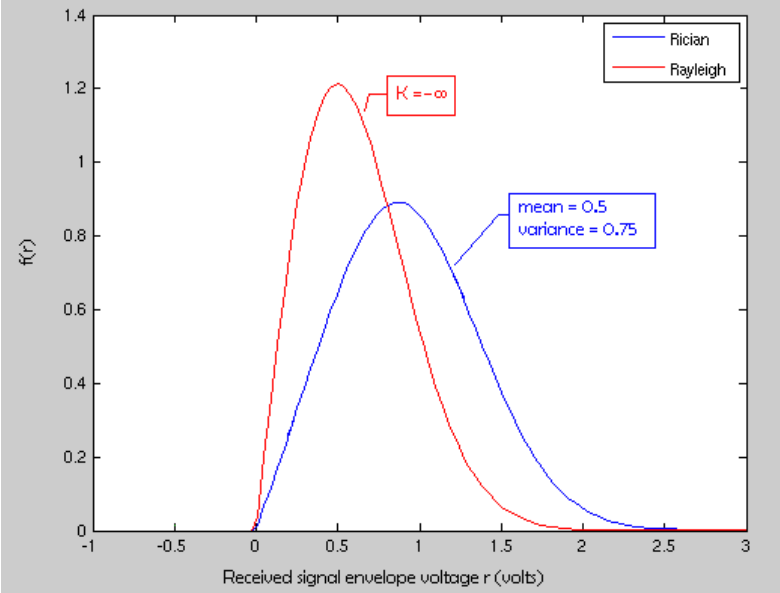

Fig. 8: Ricean and Rayleigh Probability Density Function

Ricean Fading

When there is a dominant stationary (nonfading) signal component present, such as a line-of-sight propagation path, the small-scale fading envelope distribution is Ricean. In such situation, random multipath components arriving at different angles are superimposed on a stationary dominant signal. In the presence of such a direct path or LoS, the transmitted signal can be written as

$$s(t) = \sum_{i=1}^{N} a_i \cos\left(w_c t + w_{d_i} t + \phi_i\right) + k_d \cos\left(w_c t + w_d t\right) \qquad (8)$$

where the constant k_d is the strength of the direct component, w_d is the Doppler shift along the LoS path, and w_{d_i} are the Doppler shifts along the indirect paths given by ϕ_i (Doppler shift wave expression).

The envelope, in this case, has a Ricean density function given by [13]:

$$f(r) = \frac{r}{\sigma^2} exp\left\{-\frac{r^2 + {k_d}^2}{2\sigma^2}\right\} I_o\left(\frac{r k_d}{\sigma^2}\right), \quad r \geq 0 \qquad (9)$$

where $I_o()$ is the zeroth-order modified Bessel function of the first kind.

The cumulative distribution of the Ricean random variable is given as

$$F(r) = 1 - Q\left(\frac{k_d}{\sigma}, \frac{r}{\sigma}\right), \quad r \geq 0 \tag{10}$$

where $Q(,)$ is Marcum's Q function. The Ricean distribution is often described in terms of the Ricean factor *K* defined as the ratio between the deterministic signal power (from the direct path) and the diffuse signal power (from the indirect paths). *K* is usually expressed in decibels as

$$K(dB) = 10log_{10}(\frac{k_d^2}{2\sigma^2}) \tag{11}$$

If k_d goes to zero, the direct path is eliminated and the envelope distribution becomes Rayleigh with $K = -\infty$

For MIMO channel where Ricean fading occurs, the elements of $\boldsymbol{H}$ are non-zero mean complex Gaussians. Channel matrix is expressed as [7]

$$H = \sqrt{\frac{K}{K+1}}\overline{H} + \sqrt{\frac{1}{K+1}}\tilde{H} \tag{12}$$

where,

- $\overline{\boldsymbol{H}}$ is a matrix of unit entries
- $\tilde{\boldsymbol{H}}$ are independent and i.i.d. Zero-Mean Circulant Symmetric Complex Gaussian (ZMCSCG) random variables with unit magnitude variance. Nevertheless as mentioned in [4], in the vehicular environments there is an issue of non-identical channels.
- *K* is the Ricean factor

The Ricean *K* factor is very important in completing the knowledge about the associated probability density function of a wireless channel. Indeed, to know the distribution of a wireless channel without knowing the parameters about which the distribution occurs is useless. Knowledge of the Ricean *K* factor can be useful in determining the bit error rate of a channel among other useful metrics.

In correlated Ricean fading channels, for a 2x2 MIMO systems the elements of $\boldsymbol{H}$ are given as follows:

$$H = \sqrt{\frac{K}{K+1}}\begin{bmatrix}\bar{g}_{1,1} & \bar{g}_{1,2}\\ \bar{g}_{2,1} & \bar{g}_{2,2}\end{bmatrix} + \sqrt{\frac{1}{K+1}}\begin{bmatrix}\tilde{g}_{1,1} & \tilde{g}_{1,2}\\ \tilde{g}_{2,1} & \tilde{g}_{2,2}\end{bmatrix} \tag{13}$$

Rayleigh Fading

The mobile antenna, instead of receiving the signal over one LOS path, receives a number of reflected and scattered waves. Because of the varying path lengths, the phases are random and, consequently the instantaneous received power becomes a random variable.

In the case of an unmodulated carrier, the transmitted signal at frequency reaches the receiver via a number of paths, the *i*th path having amplitude a_i and phase ϕ_i . If it is assumed that there is no direct path or LoS component, the received signal $s(t)$ can be expressed as:

$$s(t) = \sum_{i=1}^{N} a_i \, cos(w_c t + \phi_i) \qquad (14)$$

where *N* is the number of paths. The phase ϕ_i depends on the varying path lengths, changing by 2π when the path length changes by a wavelength. Therefore, the phases are uniformly distributed over [0, 2π].

When there is relative motion between the transmitter and the receiver, the effects of motion-induced frequency and phase shifts. The *i*th reflected wave with amplitude a_i and phase ϕ_i arrive at the receiver from an angle ψ_i relative to the direction for motion of the antenna.

The Doppler shift of this wave is given by:

$$w_{d_i} = \frac{w_c v}{c} cos\psi_i \qquad (15)$$

where *v* is the velocity of the mobile, *c* is the speed of light ($3 \, x \, 10^8 \, m/s$), and ψ_is are uniformly distributed over [0, 2π]. The received signal $s(t)$ can now be written as:

$$s(t) = \sum_{i=1}^{N} a_i \, cos\left(w_c t + w_{d_i} t + \phi_i\right) \qquad (16)$$

Expressing the signal in inphase and quadrature components are respectively given as:

$$I(t) = \sum_{i=1}^{N} a_i \text{con} \, (w_{d_i} t + \phi_i) \qquad (17)$$

$$Q(t) = \sum_{i=1}^{N} a_i \text{sin} \, (w_{d_i} t + \phi_i) \qquad (18)$$

The envelope R is given by:

$$R = \sqrt{|I(t)|^2 + |Q(t)|^2} \qquad (19)$$

When *N* is large, the inphase and quadrature components will be Gaussian. The probability density function (pdf) of the received signal envelope *f(r)* can be shown to be Rayleigh, given by

$$f(r) = \frac{r}{\sigma^2} exp\left\{-\frac{r^2}{2\sigma^2}\right\}, \quad r \geq 0 \qquad (20)$$

where $2\sigma^2$ is the average power. Varying the number of paths, it can be seen that the fading envelope in absence of a LoS path fits the Rayleigh distribution.

IV. CHARACTERIZATION OF MIMO CHANNELS IN VEHICULAR ENVIRONMENTS

After introducing the theoretical background beneath the fading concept in vehicular communication scenarios, this section will be focusing on the effect the fading and the environment in more realistic scenarios. This will be carried out by analysing the propagation characteristics affecting each channel response for different channel models that might be suitable for vehicular environments. Finally the measured MIMO channel is described and channel characterization criteria such as Power Delay Profile (PDP) and Path loss are more specifically explained, as they enable to characterize the radio channel out from its frequency response.

IV.1 *Channels Models for Vehicular Environments*

Radio wave propagation strongly depends on environmental influences and its modelling can be done in different manners and levels of detail. Often, too much simplistic models are chosen, which hardly represent the system characteristics in real situation. Such models typically have deterministic characteristics found in reality. However, environmental influences can hardly be modelled in deterministic manner, more advanced models with non-deterministic reception characteristics have to be applied [19]. In vehicular environments, as high speed participants are involved, the channel is strictly non-stationary.

For modelling such channels there are three different channel models:

- Block Fading Channel
- Clarke's spectrum Time Variant Fading Channel
- Non Stationary Time Variant Fading Channel

Block Fading Channel

In many wireless systems:

- Typical Doppler spreads range from 1 to 100 Hz (hence coherence time ranges from 0.01 to 1 s)
- Data rates range from 20 to 200 kbaud
- Consequently, at least L=20,000 x 0.01 = 200 symbols are affected approximately by the same fading gain

Block fading channels are characterized by having a fading behaviour constant over one whole frame. The fading coefficients are different in the next frame. This can be observed in Fig. 9, where the first sent frame presents a constant fading but completely different to the one for the second frame. On the x-axis we see the time, measured either in OFDM symbols or frames, on the y-axis there is the delay domain, and the z-axis represents the signal strength in dBm. Considering the transmission of a code word of length N, for each symbol to be affected by an independent fading gain, interleaving should be used.

The actual time spanned by the interleaved code word becomes at least NL, which means that the delay becomes very large. In security related applications, large delays are unacceptable (real time speech: 100 ms at most).

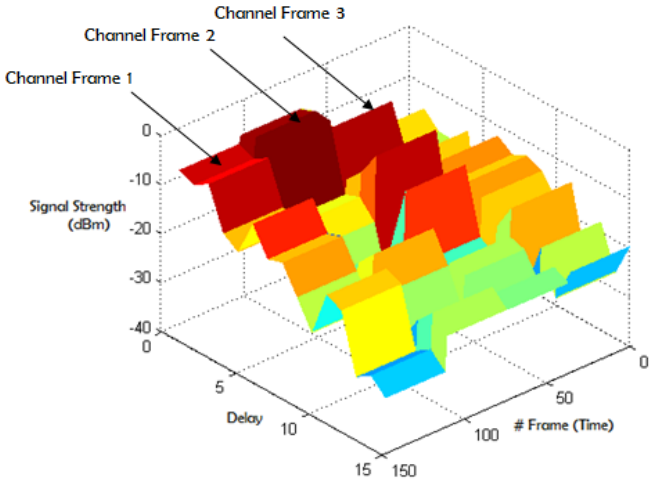

Fig. 9: Block Fading Channel

It is modelled as a sequence of independent random variables, each of which is the fading gain in a block. A code word of length n is spread over M blocks of N symbols each, so that n=NM. Each block of length N is affected by the same fading. The blocks are sent through M independent channels. The interleaver spreads the code symbols over the M blocks [20].

There are two special cases in such channel models:

- M = 1 (or N = n): the entire code word is affected by the same fading gain (no interleaving)
- M = n (or N = 1): each symbol is affected by an independent fading gain (ideal interleaving)

In such channel models the elements of the scattered components of the channel are supposed to be circularly symmetric complex Gaussian random variables.

Clarke's Spectrum Time Variant Fading Channel

A time-variant channel is an essential feature of mobile communications. The 3GPP Spatial Channel Model (SCM) [13] is well suited for simulating random-access communications. It models the channel in blocks (so-called "drops"), during which the channel only undergoes Doppler fading, but after a drop, the channel changes completely. This assumption makes it impossible to test signal processing algorithms that track the channel parameters between different snapshots. Additionally, the abrupt changes between the drops are challenging for hardware testing using channel simulators, since the device under test and the channel model need to be synchronized.

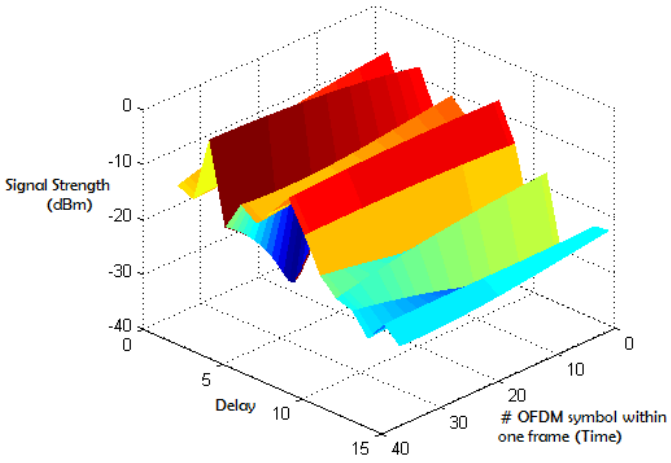

Fig. 10: Clarke's Spectrum Time Variant Fading Channel

Clarke's spectrum time-variant fading channels consider an exponential power delay profile. Each delay tap is modelled independently to the others and composed by a sum of 20 multipath contributions with Clarke's spectrum distributed Doppler shift frequencies [21, 22]. This channel model corresponds to a typical non line-of-sight situation where the receiver (Rx) is moving at a given speed. As it can be seen in Fig. 10, the fading coefficients vary already within one frame.

Non Stationary Time Variant Fading Channel

A model which lies in between the last two is the non-stationary time-variant channel model [23]. One of its main characteristics is that it considers line-of-sight between transmitter (Tx) and receiver (Rx), which both can be mobile. Also very important to notice, and shown in Fig. 11, is that it presents changes within one OFDM symbol, but in a much smoother fashion than for the one observed in the Clarke's spectrum time-variant channel model. This is because the contributions at later delays are correlated and related to a physical object.

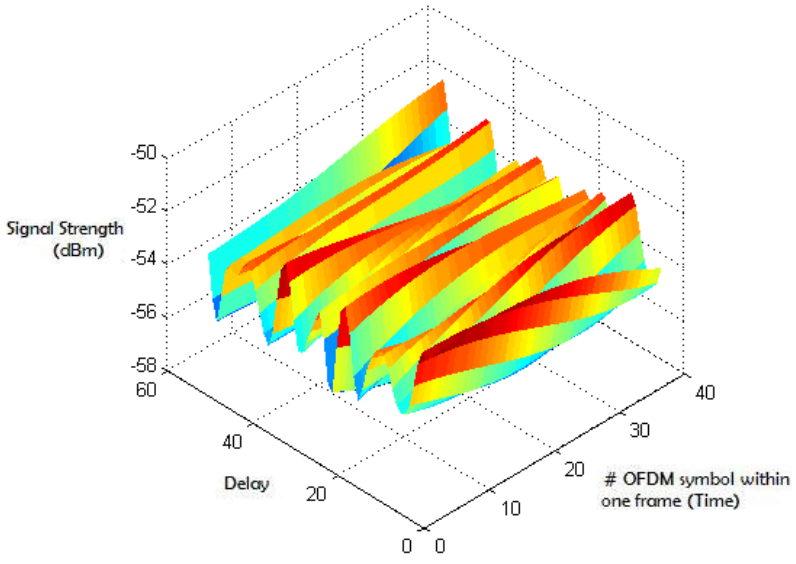

Fig. 11: Non Stationary Time Variant Fading Channel

The channel model which matches the features of the real channel from the measurement campaign carried out in Lund in 2007 will be the Non Stationary Time Variant Fading channel, as the vehicular channel to be analyzed is a Ricean Car-to-Car channel.

IV.2. *Characterization Criteria of Measured MIMO Channel in Vehicular Environments*

After the theoretical analysis on the different channel models for vehicular environments, an overview on the measured MIMO channel and on the characterization criteria is needed.

Measured MIMO Channel

Consider a communication link with M_T transmitting antennas and M_R receiving antennas.

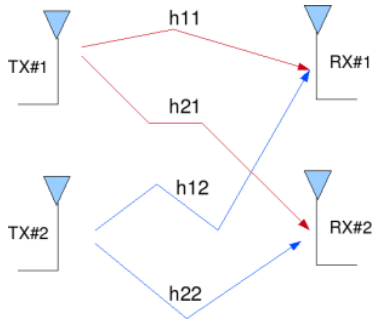

Fig. 12: MIMO channel for a $M_T = 2$ $M_R = 2$

As the Fig. 12 shows the MIMO channel will be a $M_T x M_R$ matrix containing all the $h_{M_T M_R}$ elements. In the case of the measured MIMO channel (a 4x4 MIMO channel), it has the following channel matrix structure:

$$\boldsymbol{H}(n,k) = \begin{pmatrix} h_{11}(n,k) & \cdots & h_{14}(n,k) \\ \vdots & \ddots & \vdots \\ h_{41}(n,k) & \cdots & h_{44}(n,k) \end{pmatrix} \qquad (21)$$

Some important assumptions are made:

- There is only a single user transmitting at any given time, so the received signal is corrupted by noise and by multipath generated by dynamic (other moving vehicles) and static scatterers (traffic signals).
- The communication is carried out between two transporters and the measurements were carried out with the RUSK LUND channel sounder. The cars were travelling in opposite directions, each car with a speed of 90 km/h, which results in a relative speed of 180 km/h between the two cars. This means that the channel is time-variant (see index n in Eq. 21) and that the delay of the different multipath contributions between the two vehicles (see index k in Eq. 21) has to be also be taken into account.
- The channel fading is frequency-flat within each subcarrier. This means that the channel gain can be represented by a complex number. This also means that the transmission is narrowband and the complex number, which represents fading, is constant over the considered bandwidth.

Characterization Criteria of Measured MIMO Channel

For this kind of time and delay dependent channel there are two useful characterization criteria to be taken into account: Power Delay Profile and Path Loss.

Power Delay Profile

The power delay profile (PDP) gives the intensity of a signal received through a multipath channel as a function of time delay. The time delay is the difference in travel time between multipath arrivals. The abscissa is in units of time and the ordinate is usually in decibels. It is easily measured empirically and can be used to extract certain channel's parameters such as the delay spread.

For Small Scale channel modelling, the power delay profile of the channel is found by taking the spatial average baseband impulse response of a multipath channel that is $|h_b(t;T)|^2$ over a local area.

As mentioned before, in vehicular communications the observed fading processes are non-stationary. It can be assumed that the process is stationary for a given period in time, which is labelled with the variable *k*, and then it is meaningful to represent its power spectral density as a function of time. In this sense, an estimate of the local scattering function $\hat{C}_{H[k;p,n]}$ is computed as in [25], which will allow calculating the time-variant power delay profile (PDP). The time-variant PDP is expressed as

$$PDP(k,n) = \sum_{l=1}^{L} \sum_{v=-M/2}^{\frac{M}{2}-1} \hat{C}^{l}{}_{H}[k;p,n] \qquad (22)$$

Path Loss

Path loss (or path attenuation) is the reduction in power density of an electromagnetic wave as it propagates through space. Path loss is a major component in the analysis and design of the link budget of a telecommunication system.

This term is commonly used in wireless communications and signal propagation. Path loss may be due to many effects, such as free-space loss, refraction, diffraction (when part of the radio wave front is obstructed by an opaque obstacle), reflection, aperture-medium coupling loss, and absorption (when the signal passes through media not transparent to electromagnetic waves). Path loss is also influenced by terrain contours, environment (urban or rural, vegetation and foliage), propagation medium (dry or moist air), the distance between the transmitter and the receiver, and the height and location of antennas. It also includes propagation losses caused by the natural expansion of the radio wave front in free space (which usually takes the shape of an ever-increasing sphere).

V. SPECTRAL EFFICIENCY AND OUTAGE PERFORMANCE IN RICEAN VEHICULAR COMMUNICATION CHANNELS

Once the physical features regarding to the vehicular communication channel have been fully explained, the next step will be presenting the theoretical background for the main contribution of this thesis: Spectral Efficiency and the Outage Performance Evaluation for the measured Ricean MIMO channel for vehicular environments.

V.1. *Ricean MIMO Channel for Vehicular Environments*

Recently, wireless vehicular communications for vehicle-to-vehicle (V2V) and vehicle-to-infrastructure (V2I) communications have attracted much attention [25], as they show substantial potential to enhance the traffic safety [26], efficiency, and information availability [27]. Several standards are being developed for vehicular communications, such as IEEE 802.11p WAVE and IEEE 802.20, which is designed for high-speed mobility situations, for example, for a high-speed train.

Vehicular communication poses several challenges, for example, the high mobility and the variation of the vehicular environment requires a robust communication link. Fortunately, the size of a vehicle allows it to be equipped with several antennas and to make use of MIMO systems. The well-known Orthogonal Space Time Block Coding (OSTBC) is, therefore, a suitable technique in vehicular communication, since it provides robust transmissions with very simple decoding schemes.

OSTBC has already been included in several standards, for example, Alamouti's code [5] in IEEE 802.11b and IEEE 802.11n. The receiver structure and the performance of OSTBC have been extensively studied in many works with both perfect and estimated channel state information (CSI) at the receiver. However, they are based on the assumption that the channels are independent and identically distributed (i.i.d.), but this assumption is not expected to hold in vehicular environments [4]. In a vehicular environment, both transmit and receive antennas are mounted at heights of 1–3 meters [25]. The surrounding reflectors of the signals consist of nearby vehicles and roadside buildings, which can be very close to one antenna but far from the others. The link distances are also variable from less than 1-2 meters to several tens of meters. Therefore, the channels are more likely to be non-identically distributed.

The MIMO-OFDM channel is described by its channel matrix $\boldsymbol{H}[n,k] \in \mathbb{C}^{M_{TX} x M_{RX}}$ with time index n and frequency index k. The Ricean MIMO channel both LoS component, and a scattered zero-mean component.

$$\boldsymbol{H}[n,k] = \overline{\boldsymbol{H}}[n,k] + \widetilde{\boldsymbol{H}}[n,k] \qquad (23)$$

For statistical characterization, all the columns of the channel matrix are stacked into one $L = M_{TX}xM_{RX}$ dimensional column vectors

$$h[n,k] = vec(\boldsymbol{H}[n,k]) \in \mathbb{C}^{Lx1} \qquad (24)$$

with LoS part $\bar{h}[n,k] = \mathbb{E}\{h[n,k]\}$.

In a three dimensional space the Ricean MIMO channel can be illustrated as follows:

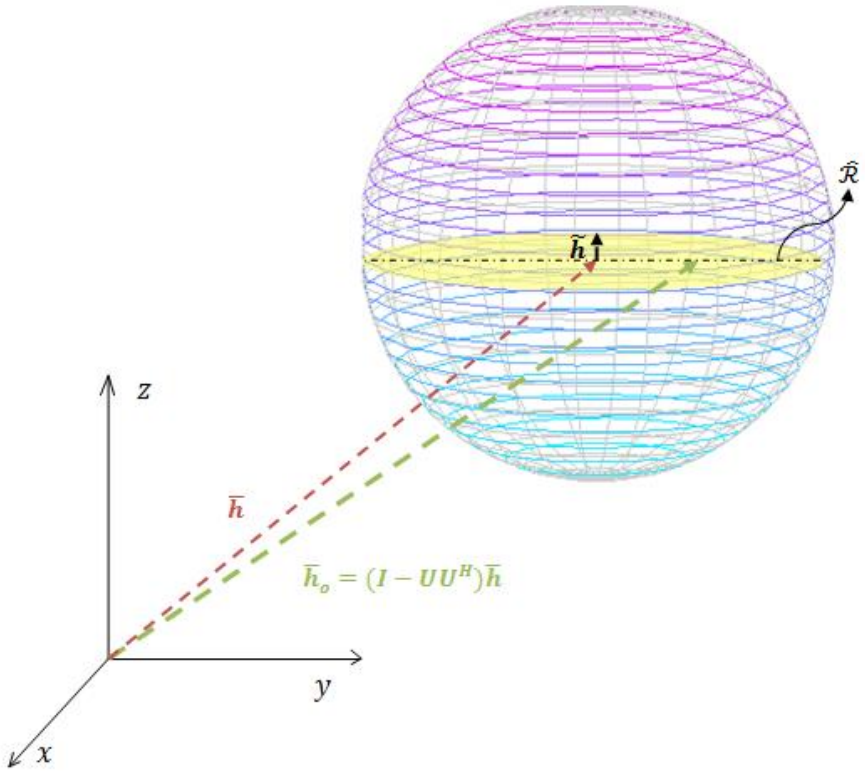

Fig. 13: Three dimensional illustration of Ricean MIMO Channel

Figure 13 shows how the scattered components generate a subspace (in light yellow). Analyzing the correlation vector $\hat{\mathcal{R}}$ of the scattered components, ones which slightly vary will be the generating vectors of the subspace, where the reliable channels will lay.

The covariance between the channel matrix elements is described in similar way by the covariance matrix

$$\phi[n,k] = \mathbb{E}\{(h[n,k] - \mu_h[n,k])(h[n,k] - \mu_h[n,k])^H\} \qquad (25)$$

where $\mu_h[n,k]$ is the mean vector of $h[n,k]$. In order to get the covariance matrix of the measured data, it has to be estimated. The covariance matrix at the time n_o

$$\hat{\phi}[n_o,k] = \frac{1}{N'}\sum_{n=n_o}^{n_o-N'}(h[n,k] - \hat{\mu}_h[n,k])(h[n,k] - \hat{\mu}_h[n,k])^H \qquad (26)$$

is estimated by averaging over N' time snapshots.

The mean vector

$$\hat{\mu}_h[n,k] = \frac{1}{N'+1}\sum_{n=n_o}^{n_o-N'} h[n,k] \quad (27)$$

For the estimation of the covariance matrix, Eq.26 and Eq.27, the estimation time *N'* has to be chosen. In [28] the stationarity time for similar highway scenario is of 23 ms. In order to stay below the stationarity time, the same as in [29] is chosen, 20ms (*N'=64*), which is about 20 wavelengths at speed of 31 m/s.

V.2. *Spectral Efficiency and Outage Performance in Vehicular Communication Channel*

For the vehicular time variant channel spectral efficiency is evaluated in terms of ergodic capacity and outage performance is usually studied by means of outage probability.

MIMO Channel Capacity

At the input of a communication system, discrete source symbols are mapped into a sequence of channel symbols. The channel symbols are then conveyed through a wireless channel that by nature is random. In addition, random noise is added to the channel symbols.

In general, it is possible that two different input sequences may give rise to the same output sequence, causing different input sequences to be confusable at the output. To avoid this situation, a non-confusable subset of input sequences must be chosen so that with a high probability, there is only one input sequence causing a particular output. It is then possible to reconstruct all the input sequences at the output with negligible probability of error. A measure of how much information that can be transmitted and received with a negligible probability of error is called the channel capacity. To determine this measure of channel potential, assume that a channel encoder receives a source symbol every T_s second.

With an optimal source code, the average code length of all source symbols is equal to the entropy rate of the source. If S represents the set of all source symbols and the entropy rate of the source is written as $H(S)$, the channel encoder will receive on average $\frac{H(s)}{T_s}$ information bits per second[1]. Assume that a channel codeword leaves the channel encoder every T_c second. In order to be able to transmit all the information from the source, there must be

$$R = \frac{H(S)T_c}{T_s} \quad (28)$$

information bits per channel symbol. The number R is called the *information rate* of the channel encoder.

[1] The **entropy** rate is a function of the statistical distribution of the source S. If the source S represents a discrete memoryless random variable, the entropy rate of the source is equal to the source entropy, and is defined as $H(S) = \mathbb{E}\{-log_b p_S\}$. It is common to use $b = 2$ and the entropy is then expressed in information bits per source symbol.

The maximum information rate that can be used causing arbitrarily low probability of error at the output is called the capacity of the channel. By transmitting information with rate R, the channel is used every T_c second. The channel capacity is then measured in bits per channel use. Assuming that the channel has bandwidth W, the input and output can be represented by samples taken $T_s = \frac{1}{2W}$ seconds apart.

With a band-limited channel, the capacity is measured in information bits per second. It is common to represent the channel capacity within a unit bandwidth of the channel. The channel capacity is then expressed in bits/s/Hz.

It is desirable to design transmission schemes that exploit the channel capacity as much as possible. Representing the input and output of a memoryless wireless channel with the random variables X and Y respectively, the channel capacity is defined as [30]

$$C = \max_{\mathrm{p(x)}} I(X;Y) \qquad (29)$$

where $I(X;Y)$ represents the *mutual information* between X and Y . Eq.29 states that the mutual information is maximized with respect to all possible transmitter statistical distributions p(x). Mutual information is a measure of the amount of information that one random variable contains about another variable. The mutual information between X and Y can also be written as

$$I(X;Y) = H(Y) - H(Y|X) \qquad (30)$$

where $H(Y|X)$ represents the conditional entropy between the random variables X and Y.
The entropy of a random variable can be described as a measure of the amount of information required on average to describe the random variable. It can also be described as a measure of the uncertainty of the random variable.

Due to Eq. 30, mutual information can be defined as the reduction in the uncertainty of one random variable due to the knowledge of the other. Note that the mutual information between X and Y depends on the properties of the channel (through a channel matrix $\boldsymbol{H}$ and the probability distribution of additive noise) and the properties of X (through the probability distribution of X).

The ergodic capacity of a fading MIMO channel with power constraint P_T can be expressed as

$$C = \mathbb{E}_H\{max_{p(x):tr(\psi)\leq P_T} I(X;Y)\} \qquad (31)$$

where σ is the covariance matrix of the transmit signal vector x. and $\mathbb{E}_\mathrm{H}$ denotes the expectation over all channel realizations The total transmit power is limited to $\mathrm{P_T}$, irrespective of the number of transmit antennas. By using Eq. 7 and the relationship between mutual information and entropy, Eq. 31 can be expanded as follows for a given $\boldsymbol{H}$**:**

$$I(x;y) = h(y) - h(y|x) \qquad (32)$$

$$I(x;y) = h(y) - h(\boldsymbol{H}x + n|x) \qquad (33)$$

$$I(x;y) = h(y) - h(n|x) \qquad (34)$$

$$I(x;y) = h(y) - h(n) \quad (35)$$

where $h(\cdot)$ in this case denotes the differential entropy of a continuous random variable. It is assumed that the transmit vector x and the noise vector n are independent.

Eq. 35 is maximized when y is gaussian, since the normal distribution maximizes the entropy for a given variance [31]. The differential entropy of a *real* gaussian vector $y = \Re^n$ with zero mean and covariance matrix $\boldsymbol{K}$ is equal to $\frac{1}{2}\log_2((2\pi e)^n \det \boldsymbol{K})$. For a *complex* gaussian vector $y = \mathbb{C}^n$, the differential entropy is less than or equal to $\log_2(\det \boldsymbol{K})$, with equality if and only if y is a circularly symmetric complex gaussian with $\mathbb{E}\{yy^H\} = \boldsymbol{K}$ [32]. Assuming the optimal gaussian distribution for the transmit vector x, the covariance matrix of the received complex vector x is given by

$$\mathbb{E}\{yy^H\} = \mathbb{E}\{(\boldsymbol{H}x + n)(\boldsymbol{H}x + n)^H\} \quad (36)$$

$$\mathbb{E}\{yy^H\} = \mathbb{E}\{\boldsymbol{H}xx^H\boldsymbol{H}^H\} + \mathbb{E}\{nn^H\} \quad (37)$$

$$\mathbb{E}\{yy^H\} = \boldsymbol{H}\psi\boldsymbol{H}^H + K^n \quad (38)$$

$$\mathbb{E}\{yy^H\} = K^d + K^n \quad (39)$$

The superscript *d* and *n* denotes respectively the desired part and the noise part of Eq. 39. The maximum mutual information of a random MIMO channel is then given by

$$I = h(y) - h(n) \quad (40)$$

$$I = log_2[det\ (\pi e(K^d + K^n))] - log_2[det\ (\pi e K^n)] \quad (41)$$

$$I = log_2[det\ (K^d + K^n)] - log_2[det\ (K^n)] \quad (42)$$

$$I = log_2[det\ ((K^d + K^n)(K^n)^{-1})] \quad (43)$$

$$I = log_2[det\ (K^d(K^n)^{-1} + I_{M_R})] \quad (44)$$

$$I = log_2[det(\boldsymbol{H}\psi\boldsymbol{H}^H(K^n)^{-1} + I_{M_R})] \quad (45)$$

When the transmitter has no knowledge about the channel, it is optimal to use a uniform power distribution [32]. The transmit covariance matrix is then given by $\psi = \frac{P_T}{M_T}\boldsymbol{I}_{M_T}$.

It is also common to assume uncorrelated noise in each receiver branch described by the covariance matrix $\boldsymbol{K}^n = \sigma^2\boldsymbol{I}_{M_T}$. Keeping in mind that the MIMO channel is described by its channel matrix $\boldsymbol{H}[n,k] \in \mathbb{C}^{M_T x M_R x}$, the ergodic (mean) capacity for a complex AWGN MIMO channel can then be expressed as [17,32]

$$C[n,k] = \mathbb{E}_H\left\{log_2\left[\det\left(\boldsymbol{I}_{M_R} + \frac{P_T}{\sigma^2 M_T}\boldsymbol{H}[n,k]\boldsymbol{H}[n,k]^H\right)\right]\right\} \quad (46)$$

where $C[n,k]$ depends on time, n, and delay bin, k. On time and delay because capacity is calculated for the channel defined within n_0 and $n_0 + 20$ ms and delay bin k.

This can also be written as

$$C[n,k] = \mathbb{E}_H\left\{log_2\left[\det\left(\boldsymbol{I}_{M_R} + \frac{\rho}{M_T}\boldsymbol{H}[n,k]\boldsymbol{H}[n,k]^H\right)\right]\right\} \quad (47)$$

where $\rho = \frac{P_T}{\sigma^2}$ is the average signal-to-noise (SNR) ratio at each receiver branch.

Further analysis of the MIMO channel capacity given in Eq. 47 is possible by diagonalizing the product matrix $\boldsymbol{H}\boldsymbol{H}^H$ by using singular value decomposition on the channel matrix $\boldsymbol{H}$ written as

$$\boldsymbol{H} = \boldsymbol{U}\boldsymbol{\Sigma}\boldsymbol{V}^H \quad (48)$$

where $\boldsymbol{U}$ and $\boldsymbol{V}$ are unitary matrices of left and right singular vectors respectively, and $\boldsymbol{\Sigma}$ is a diagonal matrix with singular values on the main diagonal. All elements on the diagonal are zero except for the first k elements. The number of non-zero singular values k equals the rank of the channel matrix. Using Eq. 48, the MIMO channel capacity can be written as

$$C[n,k] = \mathbb{E}_H\left\{log_2\left[\det\left(\boldsymbol{I}_{M_R} + \frac{\rho}{M_T}\boldsymbol{U}\boldsymbol{\Sigma}\boldsymbol{\Sigma}^H\boldsymbol{U}^H\right)\right]\right\} \quad (49)$$

After diagonalizing the product matrix $\boldsymbol{H}\boldsymbol{H}^H$, the capacity formulas of the MIMO channel now includes unitary and diagonal matrices only. It is then easier to see that the total capacity of a MIMO channel is made up by the sum of parallel AWGN SISO subchannels.

Outage Capacity

The ergodic (mean) capacity has been used as a measure for the spectral efficiency of the MIMO channel. The capacity under channel ergodicity where in Eq.31 defined as the average of the maximal value of the mutual information between the transmitted and the received signal, where the maximization was carried out with respect to all possible transmitter statistical distributions.

Another measure of channel capacity that is frequently used is outage capacity. With outage capacity, the channel capacity is associated to an outage probability. Capacity is treated as a random variable which depends on the channel instantaneous response and remains constant during the transmission of a finite-length coded block of information. If the channel capacity falls below the outage capacity, there is no possibility that the transmitted block of information can be decoded with no errors, whichever coding scheme is employed.

The probability that the capacity is less than the outage capacity denoted by C_{outage} is q. This can be expressed in mathematical terms by

$$Prb\left\{C[n,k] \leq C_{outage}[n,k]\right\} = q \quad (50)$$

In this case, Eq. 50 represents an upper bound due to fact that there is a finite probability q that the channel capacity is less than the outage capacity. It can also be written as a lower bound, representing the case where there is a finite probability $(1-q)$ that the channel capacity is higher than C_{outage}, i.e.,

$$Prb\left\{C[n,k] > C_{outage}[n,k]\right\} = 1 - q \quad (51)$$

Defining the auxiliary vector $\bar{\boldsymbol{h}}_{\boldsymbol{o}}$, the angle, γ can be calculated from the $\sin\gamma = \frac{\|\bar{h}_o\|^2}{\|\bar{h}\|^2}$

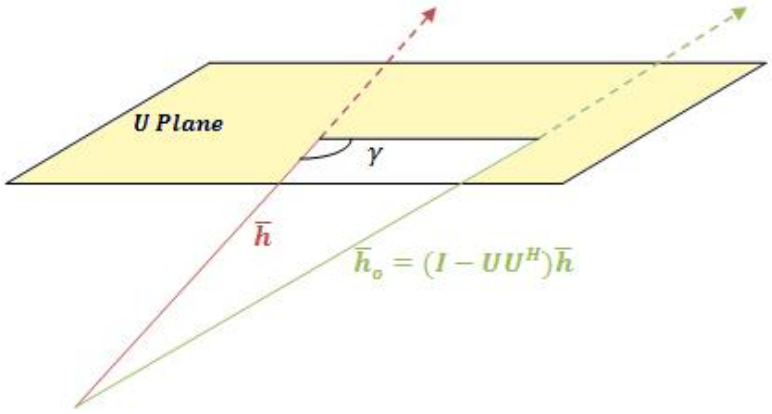

Fig. 14: Geometry of the U plane and the $\bar{h}_o$ and $\bar{h}$ vectors

The angle γ will vary with the length of $\|\bar{\boldsymbol{h}}_{\boldsymbol{o}}\|^2$, referenced in [7] as δ. So when δ is zero, γ will be 0º, which means that $\bar{\boldsymbol{h}}$ will be in the *U plane* and the channel will behave as a MIMO channel. But when δ is greater than zero, γ will also increase and there will be zero outage probability below a SNR dependent critical data rate. This means that below that data rate, the channel will behave as an AWGN channel. The greater γ is the higher the critical data rate and the more reliable is the MIMO channel.

VI. RESULTS

During this section the results of the data obtained in the measurement campaign pursued by Vienna University of Technology in Lund are going to be analyzed.

The parameter settings of the measurement campaign were the following:

Measurement configuration parameters	
Carrier frequency, f_c	5.2 GHz
Measurement bandwidth, BW	240 MHz
Delay resolution, $\Delta\tau = 1/BW$	4.2 ns
Frequency spacing, Δf	312.5 kHz
Transmit power, P_{TX}	27 dBm
Test signal length, τ_{max}	3.2 µs
Number of Tx antenna elements, M_{TX}	4
Number of Rx antenna elements, M_{RX}	4
Snapshot time, t_{snap}	102.4 µs
Snapshot repetition rate, t_{rep}	307.2 µs
Number of snapshots in time, N	32500
Number of samples in frequency domain, K	769
Recording time, t_{rec}	10 s
File size, FS	1 GB
Tx antenna height, h_{TX}	2.4 m
Rx antenna height, h_{RX}	2.4 m

Table 3: Measurement configuration parameters

VI.1. *Characterization of the Propagation Scenario*

The scenario to be analyzed will be a highway scenario. In this communication scenarios, the measurement vehicles are approaching each other from in opposite directions with different velocities v_{TX} and v_{RX}.

Highway Scenario

In this scenario both cars are crossing at 110 km/h. It takes 10 seconds to complete the measurement run.

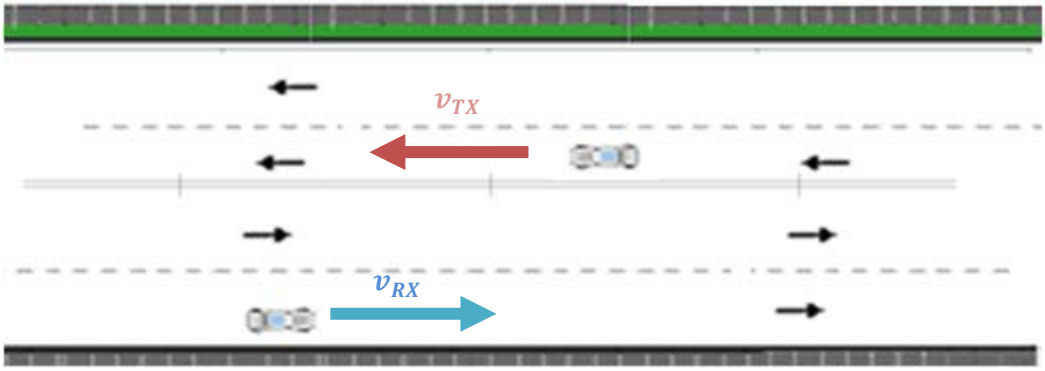

Fig. 15: Highway Scenario

In Fig. 16 contribution (1) corresponds to the LoS between Tx and Rx car. The strongest ray describes a curvature where the lowest point at 7 seconds is when the crossing between the two cars happens. In the beginning, the strongest ray has got higher delay, then as the two cars cross, the delay turns zero and as they drive away from each other the delay increases once again.

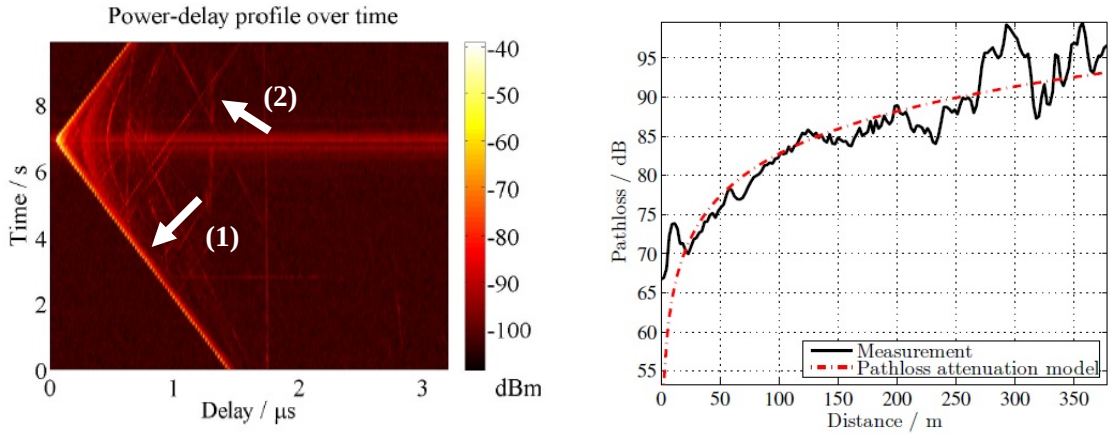

Fig. 16: Power-delay over time and Pathloss over distance profiles for the 10s measurement run [33].

Contribution (2) on the power-delay profile corresponds to some scatterers. It can be seen some reflexions parallel to the main ray which are due to the reflection of the signal on a traffic signal deployed on the measurement lane.

VI.2. *Spectral Efficiency Evaluation for the Measured Channel*

In order to evaluate spectral efficiency, ergodic capacity is going to be analyzed. As mentioned in Chapter V, the ergodic (mean) capacity is defined for every time bin, indexed as n, and delay bin, indexed as k. The snapshot time range to be analyzed is defined by the channel stationarity time. Due to the assumptions made for the estimation of the covariance matrix, the stationarity time will be the upperbound for selecting a suitable snapshot time range. Therefore and as in [33] for such an scenario, in order to stay beneath 23ms, the snapshot time range will be 20ms (with in terms of snapshots are 63 snapshots). For the time and frequency bin selection, the same time base as in [33] has been use in order to use it as a reference for comparing results.

The time bins used are 2.5 s and 7.5 s, because in [33] the both have very different diversity values, and thus a this difference should be also appreciated in the ergodic capacity. The selection of the frequency bin has been done such that both have so different values, that it can be clearly seen for ergodic capacity and critical data rate.

Fig. 17 shows the Ergodic Capacity and Critical Data Rate for n = 2.5 s and k = 628, with in frequency terms is 5.275 GHz. It must be taken in to account that the channel transfer function is obtained by comparing each frequency line in the measured data with the corresponding frequency lines in the data recorded during the calibration [34]. Thus the transfer function is normalized for each frequency line. Therefore the channel coefficients from the RUSK channel sounder related to a delay bin related will have to be multiplied with its own frequency component in order to have the correct channel transfer function in order to calculate the capacity.

The tendency of both curves is shown for different SNR values. It has to me mentioned that in order to apply this SNR sweep, the real SNR value of the measurement scenario has been calculated and its effect is undone from the channel matrix before applying the SNR sweep. The received power for each block i (meaning by block each of the runs for the different time bins), $P_T(i)$ is calculated as [35]:

$$P_T(i) = \sum_{k=1}^{769} |\boldsymbol{H}(i)|^2 \cdot P(i) \qquad (52)$$

where the transmit power $P(i)$ is being scaled by the magnitude square $|h(i)|^2$ of channel coefficients $h(i)$. In this case, as it is a 4x4 MIMO channel this magnitude square will be a mean over all the 16 channels and over the 64 snapshots. The noise level is calculated directly from the mean of the magnitude square of the channel in a delay bin range where no signal was detected.

The red line in Fig. 17 representing the critical data rate is calculated carrying out a single value decomposition of the covariance matrix and selecting the smallest vector in U corresponding to the smallest singular values in S.

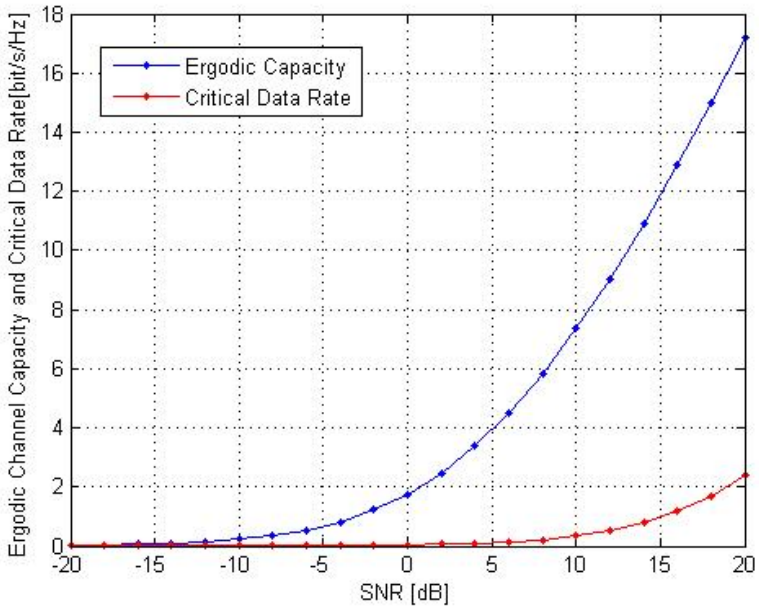

Fig. 17: Ergodic Capacity and Critical Data Rate for *n* = 2.5 s and *k* = 628 (5.275 GHz)

Comparing Fig.18 and Fig. 19 a bigger variance can be seen between the values of *n* = 7.5 s, which is directly related with a lower critical data rate in contrast to the critical data rate of *n* = 2.5 s. As the Fig. 20 will show for a SNR of 20 dB *n* = 2.5 s it is below 2 bit/s/Hz whereas *n* = 7.5 s it is below 0.5 bit/s/Hz.

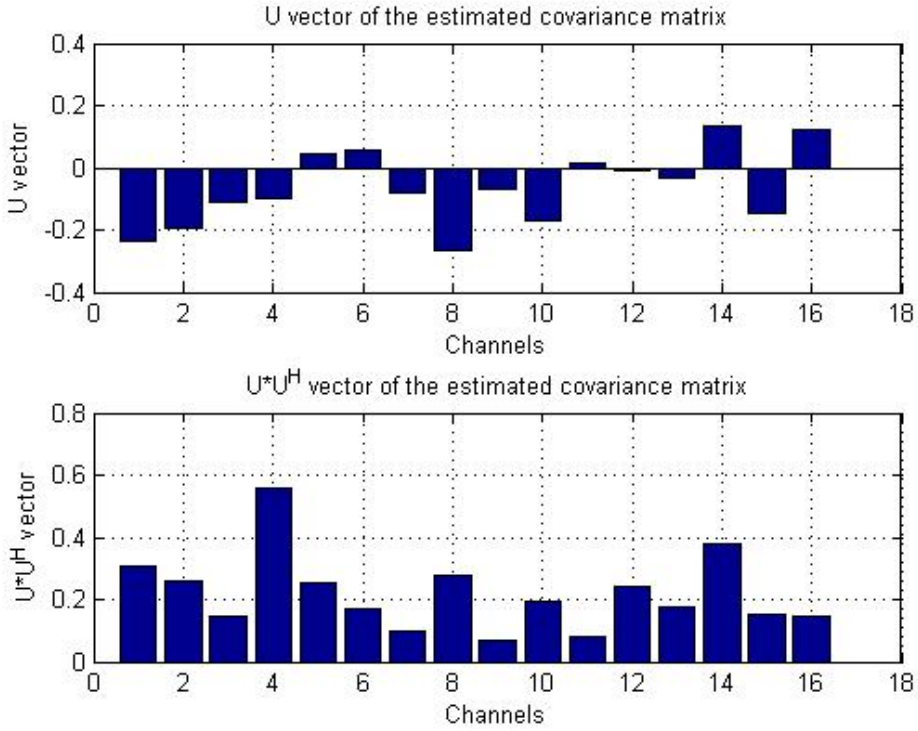

Fig. 18: Smallest *U* vector of the estimated covariance matrix for *n* = 2.5 s and *k* = 628 (5.275 GHz)

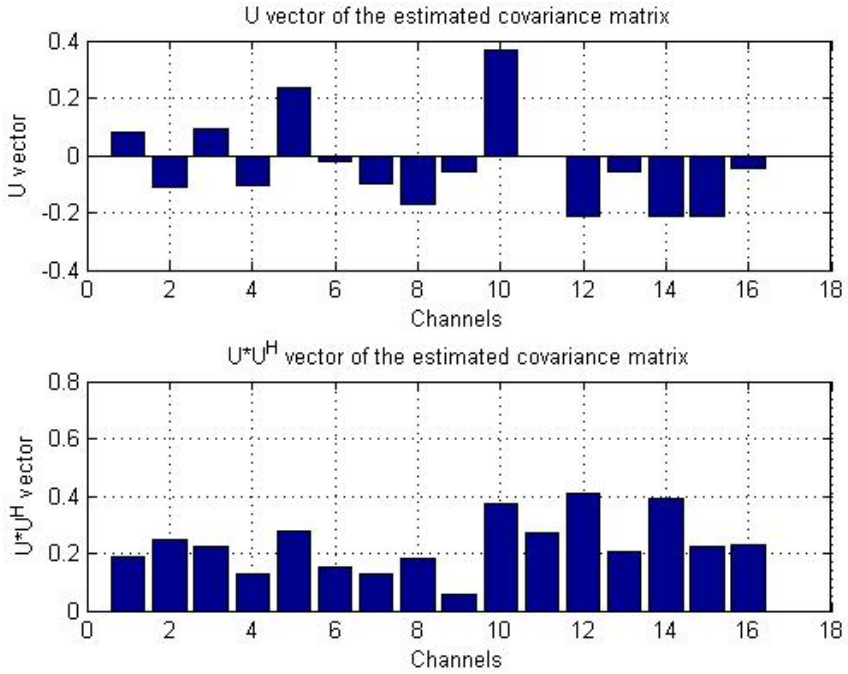

Fig. 19: Smallest U vector of the estimated covariance matrix for n = 7.5 s and k = 628 (5.275 GHz)

Parting from the vector U the auxiliary vector $\overline{h}_o$ is defined. This will be the most reliable vector, which in terms of covariance means the least variant. Converting this vector into a 16x16 matrix ($\overline{\boldsymbol{H}}_{\boldsymbol{o}}$) the capacity of this matrix is calculated, which will be the critical data rate. The blue line will be the ergodic (mean) capacity calculated out over the 64 snapshots.

In contrast with Fig. 17, Fig. 20 shows lower ergodic capacity and critical data rate. This means that there will be less number of reliable channels, able to transmit signalling information below this critical data rate with zero outage probability.

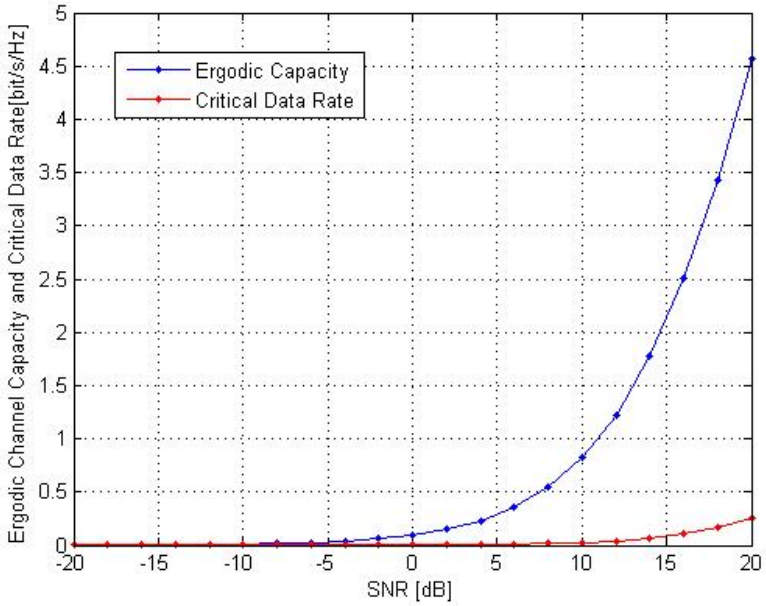

Fig. 20: Ergodic Capacity and Critical Data Rate for n = 7.5 s and k = 628 (5.275 GHz)

The outage probability analysis will be carried out in section VI.3, but it is very interesting to see the relation between this critical data rate level and the γ angle generated by the LoS channel vector, $\overline{h}$ and the auxiliary vector $\overline{h}_o$ (see Fig. 13).

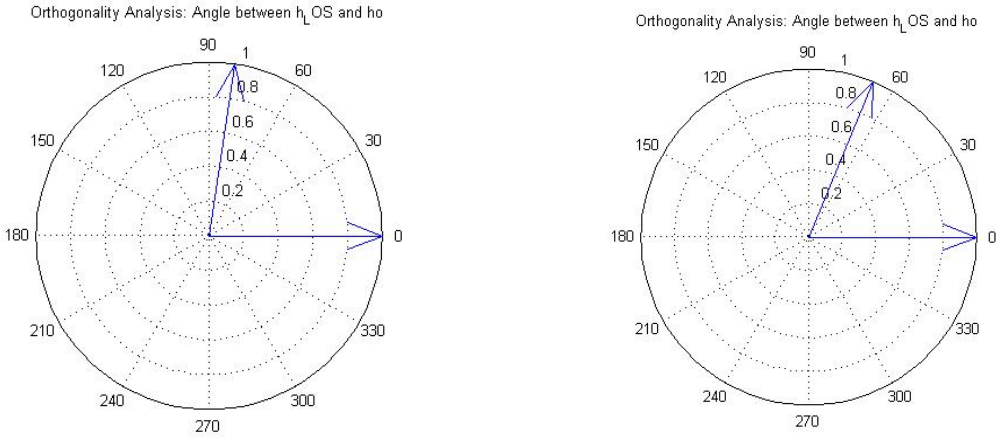

Fig. 21: Orthogonality Analysis (γ angle) for *n* = 2.5 s and *k* = 628 (LEFT) and n = 7.5 s (RIGHT)

As Fig. 21 shows $\gamma = 81º$ for n= 2.5 s whereas $\gamma = 67º$ for n= 7.5 s. The bigger the γ, the larger $\overline{h}_o$, is and greater critical data rate. This supports the results from [33] where the diversity at *n* = 2.5 s was much larger than at *n* = 7.5 s, and also the ones presented by this contribution in Fig. 17 and 20, where ergodic capacity and critical data rate for *n* = 2.5 s are larger than for *n* = 7.5 s.

And in order to evaluate the temporal progress of both ergodic capacity and critical data rate a third time instant has been selected: *n* = 10 s. Taking a fixed SNR of 20 dB (perfect power control scenario) the instantaneous ergodic capacities and critical data rates of the three instants are going to be compared.

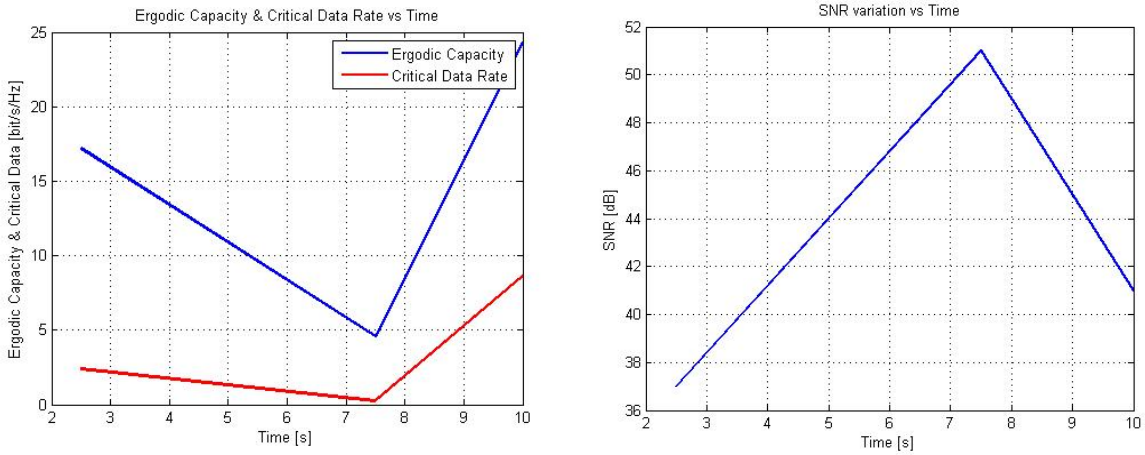

Fig. 22: Ergodic Capacity and Critical Data Rate vs. Time for a constant SNR = 20 dB (LEFT), and SNR variation with time for a constant transmit power of 27 dBm.(RIGHT)

The left Fig. 22 shows how when both cars are separated from each other before crossing (at *n* = 2.5 s), both ergodic capacity and critical data rate decrease as the cars get closer to each other.

This is because at the beginning of the measurement run, when cars are far from each other, the MIMO channels are less correlated (see Fig.18) and therefore the ergodic (mean) capacity and critical data rate will be higher. For the same SNR value, as both cars are closer to each other, the MIMO the correlation between the individual SISO channels (see Fig.19) compounding the MIMO channel will be higher (0.6) and this will make the ergodic (mean) capacity drop. That is why at 7.5 s when the cars are passing by each other the ergodic capacity and the critical data rate are lower than at 2.5 s. And finally when the cars drive apart, both parameters increase, because the more away they are from each other, the less correlated the MIMO channel is. This results are at a perfect power control scenario. But in contrast, the right Fig, 22 shows the SNR evolution with time, and here can be seen how different SNR values will affect the three time instants. The tendency is the opposite to the one of ergodic capacity.

Looking at Fig. 23, weighted ergodic capacity and Critical Data Rate vs. Time it can be concluded that as at 7.5 s there will be a higher SNR, it will not be such a big capacity drop comparing to the previous instant of the measurement run. This is because as the cars get closer, due to the direction of the main lobes of each antenna element [36], the antennas lose alignment with each other. Thus, as capacity is defined as the measure of how much information that can be transmitted and received, there will be a capacity drop at 7.5 s. Fig. 23 shows a 4 bit/s/Hz drop which is not very pronounced. This is due to the fact that the LoS component of the Ricean channel becomes stronger comparing to the scatterer contribution, which stays constant. This strengthen of the LoS will induce a higher signal level, which will keep the capacity from falling as deep as in Fig. 22.

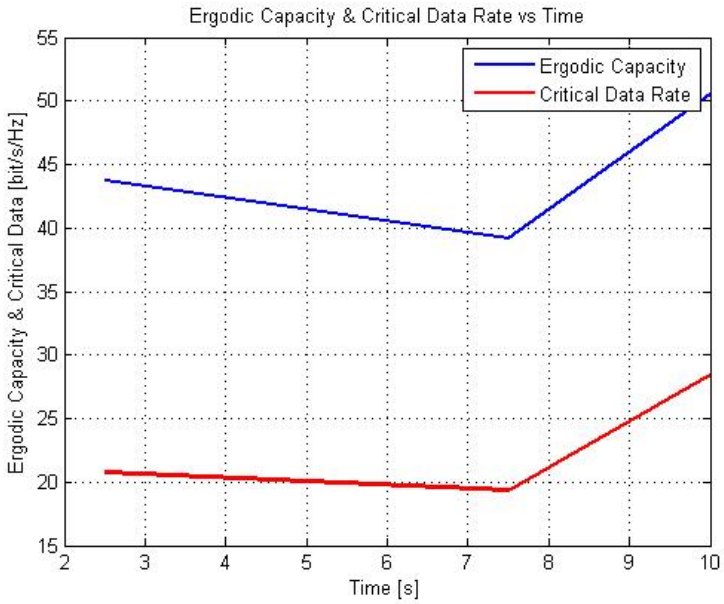

Fig. 23: Ergodic Capacity and Critical Data Rate vs. Time taken into account instantaneous SNR at each time instant.

The question that arises at this point is why the capacity is lower at 7.5 s, when the cars are crossing and as at 10 s, when cars are driving away from each other. As [37] says, the propagation should be studied in order to find the explanation for this effect. The channel with the strongest LoS component is the one that maximizes capacity. This leads to think that the channel at 7.5 s is not the one with the strongest LoS, and it is not indeed, because due to the structure of the cars there is high scattering on the metallic structure, and also the antennas are not aligned properly. But at 10 s, the cars receive from back-to-back where no metallic scatterers are deployed, and the antennas are better aligned with each other. It is then when a maximum LoS channel is depicted and this supports the results shown in Fig. 23 at 10 s, where the ergodic capacity and the critical data rate reach their maximums at 50.54 bit/s/Hz and 28.46 bit/s/Hz. respectively. Fig. 24 shows the scenario at each time.

Fig. 24: General view of the scenario and screenshots from the video of the measurement run: The Rx car approaching the Tx car, The Rx car passing by the Tx car and The Rx driving away from the Tx car (From LEFT to RIGHT)

VI.3. *Outage Performance Evaluation for the Measured Channel*

Even though the capacity distribution varies for each time and delay bin, in this section the results for the previously presented time and delay bins are going to be shown in order to keep the coherence throughout the different concepts and charts.

When looking at the capacity distribution from Fig. 25 a more symmetrical distribution can be seen, whereas Fig. 26 shows a Ricean-like distribution. Not only the shape, but also the value range of the axes is different. There are more amount of channels at lower capacities for the n = 7.5 s case as for the n = 2.5 s. And the capacity distribution also differs in the fact that there will be a higher outage probability at lower outage capacities in the case of Fig. 28. This is because at the beginning of the distribution there are larger number of channels with those initial capacities, which shows a concave parabolic increment in comparison to the second half, were a fast exponential descend is shown due to the lack of channels with such capacity values.

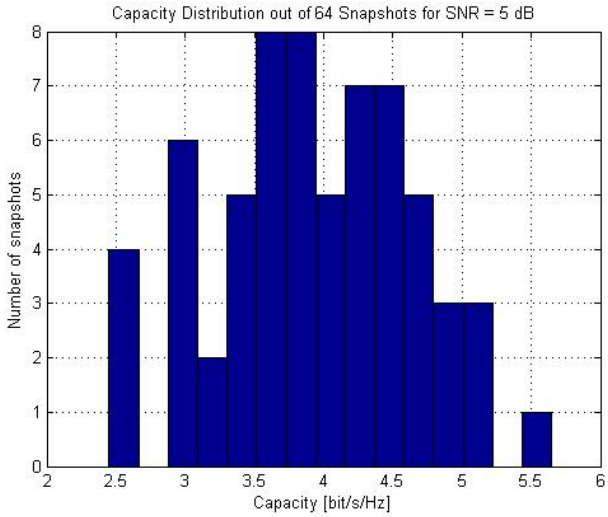

Fig. 25: Capacity Distribution for n = 2.5 s and k = 628 (5.275 GHz)

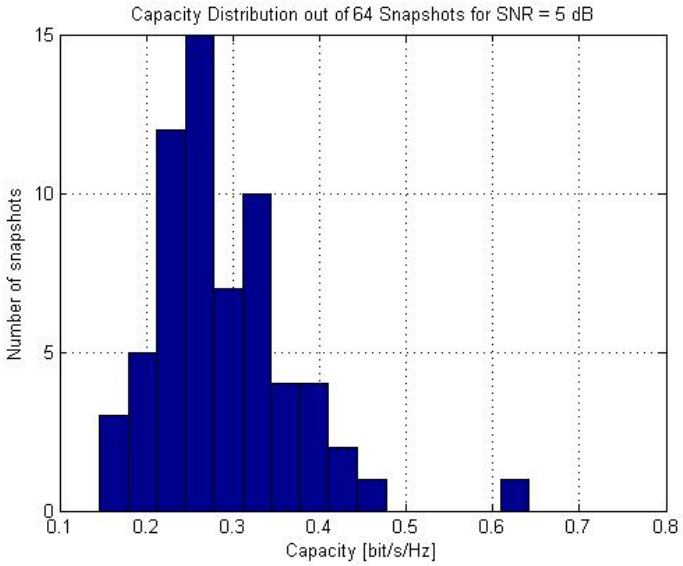

Fig. 26: Capacity Distribution for n = 7.5 s and k = 628 (5.275 GHz)

Fig. 25 shows a parabolic tendency throughout all the capacity range, which softens the outage probability.

In Fig. 27 and Fig. 28 both Outage Probability charts are shown. Note that in order to compute the probability in % the values of the y axis will have to be normalized to the amount of snapshots:

$$Prb(C \leq C_{outage}) = \frac{\{y_{value}\}}{Snapshot\ number} \cdot 100 \qquad (53)$$

The cumulative sum shown in the following figures makes it easier to understand. This way for example, given an outage capacity of 3 bits/s/Hz the outage probability for n = 2.5 s would be of 4.68%, whereas for n = 7.5 s would be higher than a 96. 87%. There would be higher outage in the less reliable case.

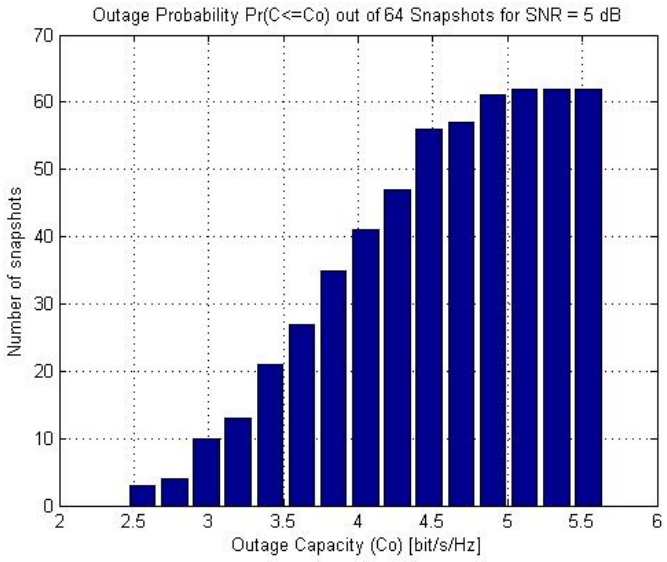

Fig. 27: Outage Probability for n = 2.5 s and k = 628 (5.275 GHz)

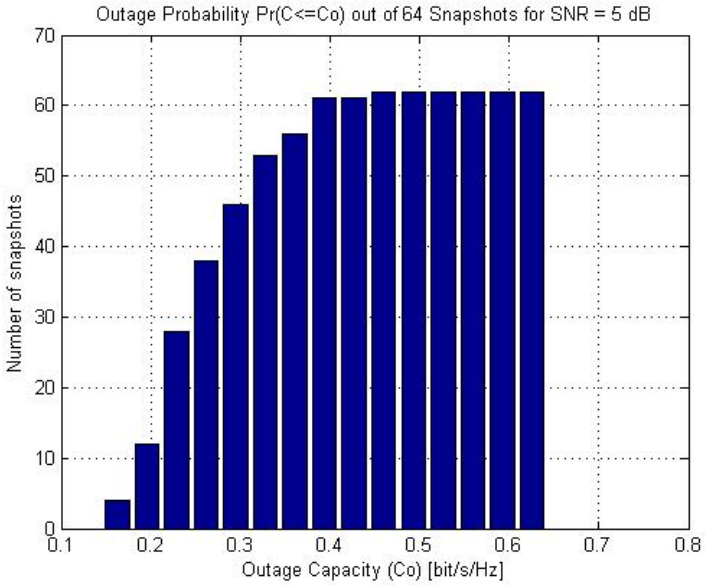

Fig. 28: Outage Probability for n = 7.5 s and k = 628 (5.275 GHz)

VII. SUMMARY AND CONCLUSIONS

In this Master Thesis the IEEE 802.11p draft amendment to the IEEE 802.11 standard to add wireless access in vehicular environments has been introduced. In Europe, a 30MHz channel is recommended for road safety applications, and further 20 MHz are suggested to be considered for future ITS expansion.

First the physical layer (PHY) structure of IEEE 802.11p has been presented, which is the same as for IEEE 802.11a and it uses OFDM transmission format. **Key parameters for the 802.11a family** of OFDM waveform include the length of the cyclic prefix or guard interval, carrier spacing, and the time intervals between channel estimates and corresponding updates to the equalization.

- In practice an OFDM symbol is typically prep ended with a circular extension called cyclic prefix that provides GI for all multiple paths following the first arrival signal. Hereby ISI and carrier orthogonality mismatches caused by multipath can be avoided. There should be ensured that the durations of the expected power-delay profiles are shorter than the GI.
- The carrier spacing can be selected so that each carrier experiences flat fading, even though the spectrum of the OFDM symbol as a whole experiences frequency selective fading. This makes easier to apply equalization in order to correct the distortion. The coherence bandwidth should be greater than the carrier spacing in order to ensure flat fading on each carrier.
- Coherence time is a metric to characterize the severe changes in the amplitude and phase of a narrow signal transmitted through the channel. It describes the interval over which the channel can be considered unchanged. In PHY IEEE 802.11a channel estimated are performed and used to correct for flat fading or individual carriers. These estimates are obtained from training sequences in the packet header and are used for the remainder of the packet. Therefore, it is very important to ensure that the duration of the packet is less than the coherence time for the corrections to remain valid.
- Doppler spread is a commonly used metric in the frequency domain is the width of the resulting spectrum, referred as the Doppler spread. To avoid the scenario where a Doppler spread signal leaks into adjacent carriers and causes interference, OFDM carrier spacing must be much larger than the maximum Doppler spread.

In order to prepare the data packet of IEEE 802.11p for high mobility vehicular communications, the bandwidth of the IEEE 802.11p PHY signal is decreased from 20MHz to 10MHz, means that all parameters in the time domain are doubled.

This bandwidth reduction is more suitable for vehicular environments, as the GI is doubled and the best performance is obtained. Moreover, no high bandwidth would be required to run safety-related applications, which are the ones that are currently under development for vehicular communications scenarios.

IEEE 802.11p Draft Amendment for Wireless Access in Vehicular Environments is meant to:

- Describe the functions and services required by WAVE-conformant stations to operate in a rapidly varying environment and exchange messages without having to join a Basic Service Set (BSS), as in the traditional IEEE 802.11 use case. IEEE 802.11p is a peer-to-peer communication scenario.
- Define the WAVE signalling technique and interference functions that are controlled by the IEEE 802.11 MAC. .

Key Amendments introduced by IEEE 802.11p	
MAC AMENDMENT	*WAVE Mode:* A station in WAVE mode is allowed to transmit and receive data frames with the wildcard BSSID value and without the need to belong to a BSS of any kind a priori. This means, two vehicles can immediately communicate with each other.
	WBSS Mode: A station uses the demand beacon. A WAVE station uses the demand window beacon, which uses the well known beacon frame and needs not to be periodically repeated, to advertise a WAVE BSS.
	Expanding the wildcard BSSID usage: Given the focus of safety as the key of WAVE, the use of wildcard BSSID is also supported even for a station already belonging to a WBSS. A station in WBSS is still in WAVE mode and can still transmit frames with the wildcard BSSID in order to reach all neighbouring stations in cases of safety concerns.
	Distributed Service: Over the air, this simply means that it is possible for data frames to be transmitted with “To DS” and “From DS” bits set to 1.
PHY AMENDMENT	*10 MHz wide channels:* it is straightforward in implementation since it mainly involves doubling of all OFDM timing parameters used in regular 20 MHz IEEE 802.11a transmissions.
	Improved receiver performance requirements: The nature of closely distributed vehicles on the road creates increased concerned for cross channel interference. In the proposed channel management policy there are Category 1 (compulsory) and Category 2(more stringent and optional) proposed.
	Improved transmission masks: Specific to the usage of IEEE 802.11p radios U.S. four spectrum masks are defined that are meant for class A to D operations.

Table 4: Key Amendments introduced by IEEE 802.11p

Regarding to channel layout, The Federal Communications Commission (FCC) of the US has allocated 75 MHz bandwidth at 5.855−5.925 GHz for the Intelligent Transportation System (ITS). This bandwidth is divided into seven channels of 10MHz, and consists of one Control Channel (CCH) and six service channels (SCH). IEEE 802.11p, in the US also called DSRC, has been adopted as the technique to offer ITS services on this frequency band. In Europe, after investigations, a 30MHz channel is recommended for road safety applications (5875−5905 MHz), and further 20 MHz (5905−5925 MHz) are suggested to be considered for future ITS expansion.

After introducing several aspects about the vehicular communication protocol and physical channel layout defined in it, the **fading in vehicular environments** has been analyzed, in order to have the background of the small and large scale fading effects affecting the vehicular communications.

Then in order to pursue a proper **characterization of MIMO channels in vehicular environments,** the way these previously mentioned fading effects affect different channel models suitable for vehicular environments has been studied. In vehicular environments, as high speed participants are involved, the channel is strictly non-stationary.

Different Channel Models for Vehicular Communications Channel modelling

Block Fading Channel	It has a fading behaviour constant over one whole frame. The fading coefficients are different in the next frame. The first sent frame presents a constant fading but completely different to the one for the second frame. In such channel models the elements of the scattered components of the channel are supposed to be circularly symmetric complex Gaussian random variables.
Clarke's spectrum Time Variant Fading Channel	It models the channel in blocks (so-called "drops"), during which the channel only undergoes Doppler fading, but after a drop, the channel changes completely. This channel model corresponds to a typical non line-of-sight situation where the receiver is moving at a given speed.
Non Stationary Time Variant Fading Channel	One of its main characteristics is that it considers line-of-sight between transmitter and receiver, which both can be mobile. it presents changes within one OFDM symbol, but in a much smoother fashion than for the one observed in the Clarke's spectrum time-variant channel model. This is because the contributions at later delays are correlated and related to a physical object.

Table 5: Different Channel Models for Vehicular Communications Channel modelling

From the presented alternatives, the channel model which matches the features of the real channel from the measurement campaign carried out in Lund in 2007 will be the Non Stationary Time Variant Fading channel, as the vehicular channel to be analyzed is a Ricean Car-to-Car channel.

For a vehicular communication channel characterization there have been two characterization criteria presented in order to analyze the transmission throughout a measurement run and the effect of the environment.

- *The power delay profile (PDP)* gives the intensity of a signal received through a multipath channel as a function of time delay. The time delay is the difference in travel time between multipath arrivals. The abscissa is in units of time and the ordinate is usually in decibels. It is easily measured empirically and can be used to extract certain channel's parameters such as the delay spread. For Small Scale channel modelling, the power delay profile of the channel is found by taking the spatial average baseband impulse response of a multipath channel that is $|h_b(t;T)|^2$ over a local area.
- *Path loss (or path attenuation)* is the reduction in power density (attenuation) of an electromagnetic wave as it propagates through space. Path loss normally includes propagation losses caused by the natural expansion of the radio wave front in free space (which usually takes the shape of an ever-increasing sphere), absorption losses (sometimes called penetration losses), when the signal passes through media not transparent to electromagnetic waves, diffraction losses when part of the radio wave front is obstructed by an opaque obstacle, and losses caused by other phenomena.

And finally the main contribution of this thesis: **Spectral efficiency and Outage Performance in Ricean Vehicular Communication Channels.** The MIMO channel has been geometrically described by its channel matrix $\boldsymbol{H}[n,k] \in \mathbb{C}^{M_{TX}xM_{RX}}$ with time index *n* and frequency index *k*. It has also got, apart from the LoS component, a scattered zero-mean component.

Analyzing the correlation vector $\hat{\mathcal{R}}$ of the scattered components, ones which slightly vary will be the generating vectors of the subspace, where the reliable channels will lay. But as the correlation of only the scattered components is meaningful, the mean LoS component has to be subtracted. Thus it will be more interesting in this case to analyze the covariance of the whole Ricean channel. The covariance between the channel matrix elements is described in similar way by the covariance matrix. For the estimation of the covariance matrix, the right estimation time has been chosen (20 ms) always below the stationarity time.

Once the covariance matrix is calculated, via single value decomposition of it is done, selecting the smallest vector in U corresponding to the smallest singular values in S (Fig. 18 and 19). And from this U vector the critical data rate and the γ angle (between the LoS component and itself) are calculated.

If $\gamma > 0^{\circ}$ there will be a critical data rate below which a zero outage transmission is possible. And the bigger this angle is, the higher the critical data rate is, and also the higher is the ergodic capacity, as it is shown in the results (Fig. 17, 20 and 21). A higher ergodic capacity means a higher spectral efficiency for a certain SNR value. So by spectral efficiency means the bigger γ, the more efficient the channel will be. Results also show that even if the capacity decreases as the the MIMO channel correlation increases, the tendency of the ergodic capacity and critical data rate over time is not as descendent as it could be with perfect power control (see Fig. 22 LEFT) due to the strength of the LoS component when both cars are passing by each other at n = 7.5 s (see Fig. 23). And finally the maximum capacity is reached at the maximum LoS channel, which occurs at 10 s, when cars are driving from each other with Tx-Rx antennas are better aligned and no metallic scatterers at the rear structure of the cars. The maximum values for a constant tranmit power of 27 dBm are 50.54 bit/s/Hz and 28.46 bit/s/Hz for ergodic capacity and critical data rate, respectively.

Regarding Outage Performance, the capacity distribution over the 64 snapshots has been analyzed. For the more reliable channel the distribution follows symmetric shape of a concave down parabola, whereas for the least reliable channel has got a Ricean envelope tendency (Fig. 25 and 26). When analyzing the cumulative sum (Fig. 27 and 28) it is more clearly shown that the more reliable channel has got lower outage probability for its initial outage capacities, as the less reliable one, which has got large outage probabilities for its initial outage capacity values.

Vehicular communication brings forward several challenges, for example, the high mobility and the variation of the vehicular environment requires a robust communication link. Fortunately, the size of a vehicle allows it to be equipped with several antennas and to make use of multiple-input multiple-output (MIMO) systems. Spectral efficiency has shown a maximal ergodic capacity at maximum LoS channel and a capacity drop of 4 bit/s/Hz when the cars are crossing each other due to the misalignment of the antennas and the correlation of the channel matrix at 7.5 s. This could be solved with more omnidirectional antennas and calibrating the antennas taking into account the cars structure, so the scatterers don't have such a impact. Adding these features to the fact that zero outage signalling is possible below the critical data rate, makes MIMO a eligible technology for vehicular communications. Nevertheless further work has to be done in the area of interference analysis and managing in vehicular environments. This measurement campaign had only one transmitter so the SNR has been analyzed. Nevertheless in a multi-user scenario analysing the signal to interference plus noise ratio (SINR) would be an interesting feature of study.

ACKNOWLEDGEMENT

This Master Thesis is in the frame of the postgraduate studies "Master en Tecnologías, Redes y Sistemas de Comunicaciones" from the Universidad Politécnica de Valencia, which were funded by "Programa de becas para studios de máster en España" of "Obra Social La Caixa".

The paper **"***Capacity Evaluation of Measured Vehicle-to-Vehicle Radio Channels at 5.2 GHz***"** based on the research and results of this Master Thesis is review-dependent for proceeding of Workshop on Vehicular Connectivity at IEEE ICC 2010 in Cape Town.

The author thanks Héctor Esteban Gonzalez, as director from the postgraduate program for supporting her on her idea of pursuing the second semester of the program abroad, her tutors from Valencia, especially Gema Piñero Sipán for her helpful availability, and last but not least her tutors from Vienna University of Technology, Christoph Mecklenbräuker, for giving her the chance of being part of the REALSAFE and DRIVEWAY projects, and Alexander Paier for being there always ready for discussion. Thank you both for pushing me towards perfection.

BIBLIOGRAPHY

[1] "Part 11: Wireless LAN medium access control (MAC) and physical layer (PHY) specifications, Amendment 7: Wireless Access in Vehicular Environments" IEEE Std. 802.11p, 2009 (D9.0).

[2] A. J. Paulraj, D. A. Gore, R. U. Nabar and H. Bölcskei, "An overview of MIMO Communications" in Proceedings of the IEEE, vol. 92, no. 2, pp. 198-218, Feb. 2004.

[3] V. Tarokh, H. Jafarkhani, and A. R. Calderbank, "Space-time block codes from orthogonal designs," IEEE Transactions on Information Theory, vol. 45, no. 5, pp. 1456–1467, July 1999.

[4] J. He and P. Yuen Kam, "Orthogonal Space-Time Block Codes in Vehicular Environments: Optimum Receiver Design and Performance Analysis" in Proceedings of the EURASIP Journal on Wireless Communications and Networking, Hindawi Publishing Corporation, March 2009.

[5] S. M. Alamouti, "A simple transmit diversity technique for wireless communications," IEEE Journal on Selected Areas in Communications, vol. 16, no. 8, pp. 1451–1458, 1998.

[6] P. Almers, et al., "Survey of Channel and Radio Propagation Models for Wireless MIMO Systems" EURASIP Journal on Wireless Communications and Networking, Volume 2007 (2007)

[7] R. U. Nabar, H. Bölcksei and A. J. Paulraj, "Diversity Performance of Ricean MIMO Channels" in Proceedings of the ITG Workshop on Smart Antennas, Munich, Germany, March 2004.

[8] A. F. Molisch, "Wireless Communications", John Wiley & Sons, pp.65-71, 89-92, 2005.

[9] K. Mizutani and R. Kohno, "Analysis of multipath fading due to two-ray fading and vertical fluctuation of the vehicles in ITS inter-vehicle communications" in Proceedings of The IEEE 5th International Conference on Intelligent Transportations Systems, 2002.

[10] T. S. Rappaport, "Wireless Communications. Principles & Practice", Prentice Hall, pp. 102-106; 167-185, 1996.

[11] R. U. Nabar, H. Bölcksei and A. J. Paulraj, "Diversity and Outage Performance in Space-Time Block Coded of Ricean MIMO Channels" in Proceedings of IEEE Transactions Wireless Communications, vol. 4, no. 5, pp. 2519-2532, September 2005.

[12] "Part 11: Wireless LAN medium access control (MAC) and physical layer (PHY) specifications, high-speed physical layer in the 5GHz band," IEEE Std. 802.11a, 1999 (R2003).

[13] D. Tse and P. Viswanath "Fundamentals of Wireless Communication", pp. 35-37, Cambridge University Press, 2005.

[14] L. Cheng, et al., “A measurement study of time-scaled 802.11a waveforms over the mobile-to-mobile vehicular channel at 5.9 GHz”, IEEE Communications Magazine, pp. 84-91, May 2008.

[15] D. Jiang and L. Delgrossi, “IEEE 802.11p: Towards an International Standard for Wireless Access in Vehicular Environments”, in Proceedings of Vehicular Technology Conference, 2008. VTC Spring 2008,

[16] L. Le, W. Zhang, A. Festag, and R. Baldessari, “Analysis of approaches for channel allocation in car-to-car communication”, in First international conference on the internet of things (IOT 2008) Workshop, 2008.

[17] G.J. Foschini, M.J. Gans, “On limits of wireless communication in a fading environment when using multiple antennas,” *Wireless Personal Communications*, vol. 6, no. 3, pp. 311-335, Mar. 1998.

[18] D. Gesbert, H. Bölcskei, D. J. Gore, A. J. Paulraj, “Outdoor MIMO wireless channels: Models and Performance prediction,” *IEEE Trans. Commun.*, vol. 50, no. 12, pp. 1926–1934, Dec. 2002.

[19] F. Schmidt and M. Killat, “Vehicle-to-Vehicle Communications: Reception and Interference of Safety-Critical Messages”, Information Technology no. 50, pp. 230-237, Oldenbourg Wissenschaftsverlag, 2008.

[20] E. Biglieri, G. Caire and G. Taricco, “Limiting performance of block-fading channels with multiple antennas”, in proceedings of IEEE Transactions on Information Theory, vol. 47, pp. 1273-1289, May 2001.

[21] Y. R. Zheng and C. Xiao, “Simulation models with correct statistical properties for Rayleigh fading channels," Communications, IEEE Transactions on, vol. 51, pp. 920-928, June 2003.

[22] T. Zemen and C. Mecklenbräuker, “Time-variant channel estimation using discrete prolate spheroidal sequences," Signal Processing, IEEE Transactions on, vol. 53, pp. 3597-3607, Sept. 2005.

[23] J. Karedal, F. Tufvesson, N. Czink, A. Paier, C. Dumard, T. Zemen, C. Mecklenbräuker, and A. Molisch, “A geometry-based stochastic MIMO model for vehicle-to-vehicle communications," Wireless Communications, IEEE Transactions on, vol. 8, pp. 3646-3657, July 2009.

[24] A. Paier, J. Karedal, N. Czink, H. Hofstetter, C. Dumard, T. Zemen, F. Tufvesson, C. F. Mecklenbräuker, and A. F. Molisch, “First results from car-to-car and car-to-infrastructure radio channel measurements at 5.2GHz,” in International Symposium on Personal, Indoor and Mobile Radio Communications (PIMRC 2007), pp. 1–5 , 3-7 Sep. 2007.

[25] W. Xiang, P. Richardson, and J. Guo, “Introduction and preliminary experimental results of wireless access for vehicular environments (WAVE) systems,” in Proceedings of the 3rd Annual International Conference on Mobile and Ubiquitous Systems: Networking and Services (MOBIQW '06), pp. 1–8, San Jose, Calif, USA, July 2006.

[26] G. Moniak, M. Berbineau, and J. F. Pardonche, “Robust and high data rate transmissions for security between a bus and a control center,” in Proceedings of the 60th IEEE Vehicular Technology Conference (VTC '04), vol. 2, pp. 1377–1381, Los Angeles, Calif, USA, September 2004.

[27] S. Eichler, “Performance evaluation of the IEEE 802.11p WAVE communication standard,” in Proceedings of the 66th IEEE Vehicular Technology Conference (VTC '07), pp. 2199–2203, Baltimore, Md, USA, September-October 2007.

[28] A. Paier, T. Zemen, L. Bernadó, G. Matz, J. Karedal, N. Czink, C. Dumard, F. Tufvesson, A. F. Molisch, and C. F. Mecklenbräuker, “Non-WSSUS vehicular channel characterization in highway and urban scenarios at 5.2GHz using the local scattering function,” in International Workshop on Smart Antennas (WSA 2008), 26-27 Feb. 2008, pp. 9–15.

[29] A. Paier, T. Zemen, J. Karedal, N. Czink, C. Dumard, F. Tufvesson, C. F. Mecklenbräuker and A. F. Molisch, “Spatial Diversity and Spatial Correlation Evaluation of Measured Vehiche-to-Vehicle Radio Channels at 5.2 GHz,” in 2009 IEEE 13th DSP Workshop & 5th SPE Workshop, IEEE Catalog, (2009), ISBN: 978-1-4244-3677-4

[30] J. G. Proakis, “Digital Communications,” McGraw-Hill, Inc., 1995.

[31] T. M. Cover, J. A. Thomas, “Elements of Information theory,” John Wiley & Sons, Inc., 1991.

[32] I. Telatar, “Capacity of multi-antenna Gaussian channels,” AT&T Technical Memorandum, 1995.

[33] A. Paier, J. Karedal, N. Czink, H. Hofstetter, C. Dumard, T. Zemen, F. Tufvesson, A. F. Molisch and C. F. Mecklenbräuker, “Car-to-Car radio channel measurements at 5 GHz: Pathloss, power-delay profile, and delay-Doppler sprectrum,” in Proceedings of IEEE International Symposium on Wireless Communication Systems, Trodtheim, Norway, October 2007.

[34] G. Eriksson, S. Linder, K. Wiklundh, P. D. Holm, P. Johannson, F Tufvensson and A. Molisch, “Urban Peer-to-Peer MMO Channel Measurements and Analysis at 300 MHz, ” IEEE Military Communications Conference, (2008), pp.1-8

[35] C. F. Mecklenbräuker and N. Goertz, “The flyby-Channel and upper limits for its “Capacity”, Institute of Communications and Radio-Frequency Engineering, Viena University of Technology, November 2008.

[36] A. Paier, J. Karedal, N. Czink, H. Hofstetter, C. Dummard, T. Zemen, F. Tufvesson, C. F. Mecklenbräuker and A. F. Molisch, “First Results from Car-to-Car and Car-to-Infrastructure Radio Channel Measurements at 5.2 GHz”, in Proceedings of The 18th Annual IEEE International Symposium on Personal, Indoor and Mobile Radio Communications (PIMRC’07), 2007

[37] E. Bonek, M. Herdin, W. Weichselberger and H. Özcelik, “MIMO – Study Propagation First!“ Institute of Communications and Radio-Frequency Engineering, Viena University of Technology, November 2004.